ACSNANO

www.acsnano.org

REVIEW

Magnetic Measurement and Stimulation of Cellular and Intracellular Structures

Xian Wang, Junhui Law, Mengxi Luo, Zheyuan Gong, Jiangfan Yu, Wentian Tang, Zhuoran Zhang, Xueting Mei, Zongjie Huang, Lidan You, and Yu Sun*

Cite This: *ACS Nano* 2020, 14, 3805–3821

Read Online

ACCESS | Metrics & More | Article Recommendations

ABSTRACT: From single-pole magnetic tweezers to robotic magnetic-field generation systems, the development of magnetic micromanipulation systems, using electromagnets or permanent magnets, has enabled a multitude of applications for cellular and intracellular measurement and stimulation. Controlled by different configurations of magnetic-field generation systems, magnetic particles have been actuated by an external magnetic field to exert forces/torques and perform mechanical measurements on the cell membrane, cytoplasm, cytoskeleton, nucleus, intracellular motors, *etc.* The particles have also been controlled to generate aggregations to trigger cell signaling pathways and produce heat to cause cancer cell apoptosis for hyperthermia treatment. Magnetic micromanipulation has become an important tool in the repertoire of toolsets for cell measurement and stimulation and will continue to be used widely for further explorations of cellular/intracellular structures and their functions. Existing review papers in the literature focus on fabrication and position control of magnetic particles/structures (often termed micronanorobots) and the synthesis and functionalization of magnetic particles. Differently, this paper reviews the principles and systems of magnetic micromanipulation specifically for cellular and intracellular measurement and stimulation. Discoveries enabled by magnetic measurement and stimulation of cellular and intracellular structures are also summarized. This paper ends with discussions on future opportunities and challenges of magnetic micromanipulation in the exploration of cellular biophysics, mechanotransduction, and disease therapeutics.

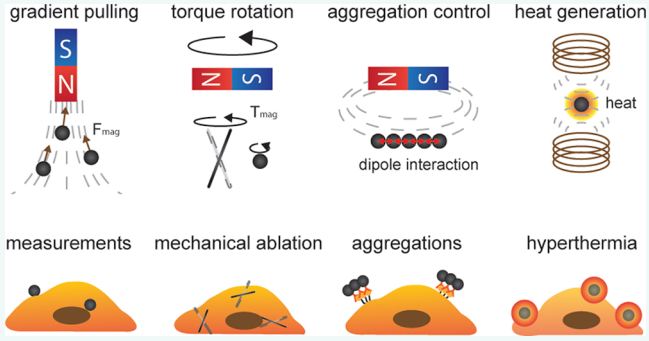

KEYWORDS: *magnetic micromanipulation, cell mechanics, intracellular biophysics, micro/nanorobotics, hyperthermia, mechanosensation, mechanotransduction, cell mechanical stimulation, cell apoptosis*

In the human body, cells are continuously subjected to mechanical forces, such as shear from blood flow and compressive/tensile forces from neighboring cells and the extracellular matrix.[1] Cells adapt to the mechanical force-abundant microenvironment *via* mechanically sensitive receptors and ion channels,[2] cytoskeleton,[3] and intracellular organelles that are responsive to force stimulations (*e.g.*, lysosomes,[4,5] endoplasmic reticulum,[6] and nucleus[7,8]). The ability of cells to deform and respond to mechanical forces is critical for embryonic development and for homeostasis in adult tissues and organs.[9] The mechanical property of the cell and intracellular organelles defines the cellular response to the mechanical forces exerted by the cell's microenvironment. Measuring the properties of cellular and intracellular structures enables a better understanding of the mechanisms of tissue development and disease progression,[10] and deciphering how cells sense and respond to mechanical signals.[11] The study of mechanical stimulation on cellular structures and downstream effects is key to understanding cell mechanobiology, such as cell migration and mitosis,[3] DNA stability,[12] and intracellular transportations,[13,14] and its relevance in diseases such as cancer.[15]

Significant progress has been made in the development of the techniques, driven by magnetic,[16] optical,[17] acoustic,[18] electrical,[19] fluidic, and other actuation fields,[20] for measurement and stimulation of cellular and intracellular structures.

Received: February 3, 2020
Accepted: March 30, 2020
Published: March 30, 2020

https://dx.doi.org/10.1021/acsnano.0c00959
ACS Nano 2020, 14, 3805–3821

For force generation, magnetic, acoustic, and electrical fields can produce forces as large as hundreds of picoNewton to several nanoNewton for manipulation, while the optical field is typically used to generate tens of picoNewton forces to avoid high laser intensity-induced damage to cellular structures. Compared with optical, acoustic, and electrical fields, measurement and stimulation using the magnetic field have the advantages of large force output, high precision, and deep-tissue penetration. Over the past decade, magnetic micromanipulation has undergone significant advances, for the measurement and stimulation of cellular and intracellular structures.[21,22] Existing review papers in the literature focus on fabrication and position control of magnetic particles/structures (often termed micronanorobots)[23,24] and the synthesis and functionalization of magnetic particles.[25−27] Differently, this paper reviews the principles and systems of magnetic micromanipulation specifically for cellular and intracellular measurement and stimulation. Discoveries enabled by magnetic measurement and stimulation of cellular and intracellular structures are also summarized. This paper ends with discussions on future opportunities and challenges of magnetic micromanipulation in the exploration of cellular biophysics, mechanotransduction, and disease therapeutics.

Principles of Magnetic Micromanipulation. *Magnetic Force and Dynamics. Magnetic Particles.* Magnetic particles can be categorized into paramagnetic particles and ferromagnetic particles. Paramagnetic particles are made of paramagnetic materials (*e.g.*, gadolinium) which generate a magnetic moment in the presence of a magnetic field.[37] Utilizing their low susceptibility, paramagnetic particles are commonly used in medicine as MRI contrast agents. Ferromagnetic particles are made of iron, nickel, cobalt, and their compounds or alloys.[37] With a high susceptibility, ferromagnetic particles are magnetized and actuated through controlling the magnetic field. For sufficiently small ferromagnetic particles, the magnetization of these particles can randomly flip directions under the influence of temperature. This phenomenon is called superparamagnetic.[38] Ferromagnetic particles remain magnetized, while superparamagnetic particles lose magnetization quickly (*i.e.*, 1−10 ns) after the removal of the magnetic field. Compared with ferromagnetic particles, the magnetic moment of paramagnetic particles is significantly lower, due to their much lower susceptibility. Thus, ferromagnetic particles are more commonly used for the measurement and stimulation of cellular and intracellular structures.

Magnetic particles ranging from 100 nm to 10 μm are widely used for cellular and intracellular measurement and stimulation. The wide size range allows the magnetic particles to attach to a variety of targets, such as proteins, intracellular organelles, virus, and cells.[39,40] Smaller sized particles (*e.g.*, <1 μm) were shown to be more easily internalized into cells through endocytosis or microinjection,[22] with less toxicity to cells.

Functionalization of magnetic particles increases biocompatibility and selectivity to target structures and reduces unintentional aggregations. To avoid exposing iron on the surface of particles for biocompatibility, magnetic microparticles typically consist of a magnetic core made from iron or nickel with a biological matrix made from starch or dextran on the surface.[41] For targeting specific proteins or cellular structures, magnetic particles can be functionalized by the carboxylic or amine group for further integration with antibodies.[42] For avoiding particle aggregation and nonspecific bindings, polyethylene glycol (PEG)[43] and nitrilotriacetic acid (NTA)[44] are often used as a blocking functionalized layer on the particle's surface.

Magnetic Force. For a magnetic particle in a magnetic field, the magnetic force that the particle subjects to is determined by its induced magnetic moment and the gradient of the magnetic field, namely

$$\mathbf{F} = \nabla(\mathbf{m}\cdot\mathbf{B}) \tag{1}$$

where $\mathbf{F}$ is the magnetic force, $\mathbf{m}$ is the magnetic moment, and $\nabla\mathbf{B}$ is the gradient of the magnetic field. The induced magnetic moment of a particle depends on the magnetic flux density $\mathbf{B}$, the magnetic permeability of the material μ, and the total volume of the magnetic material V within the field, namely

$$\mathbf{m} = \frac{3V}{\mu_0}\left(\frac{\mu-\mu_0}{\mu+2\mu_0}\right)\mathbf{B} \tag{2}$$

When the size of the particle scales down, the magnetic moment $\mathbf{m}$ scales down with volume; thus, the magnetic force scales down by a factor of 3.

Generation of a relatively large magnetic force is often required to perform mechanical measurement or stimulation tasks inside the cell. According to eq 1, magnetic particles with a large amount of ferrite are often used for large magnetic moment, and a high magnetic-field gradient is generated through using sharp magnetic poles[21] or through using strong permanent magnets.[28]

When multiple magnetic particles are present in the workspace, each particle is also subjected to a magnetic force caused by other magnetic particles. The interparticle force between two magnetic particles (particles i and j) is

$$\mathbf{F}_{ij} = \frac{3\mu_0}{4\pi\hat{\mathbf{r}}^4}((\hat{\mathbf{r}}\times\mathbf{m}_i)\times\mathbf{m}_j + (\hat{\mathbf{r}}\times\mathbf{m}_j)\times\mathbf{m}_i - 2\hat{\mathbf{r}}(\mathbf{m}_i\cdot\mathbf{m}_j) + 5\hat{\mathbf{r}}((\hat{\mathbf{r}}\times\mathbf{m}_i)\cdot(\hat{\mathbf{r}}\times\mathbf{m}_j))) \tag{3}$$

where r is the distance between two particles and $\hat{\mathbf{r}}$ is a unit vector between the centers of mass of particle i and that of j. These magnetic interaction forces cause the particles to attract to each other and form an aggregate.

Magnetic Torque. In a rotating magnetic field, the direction of the magnetic flux density $\mathbf{B}$ changes, and the magnetic moment of a particle aligns itself toward the direction of magnetic flux density, as the magnetic torque follows

$$\mathbf{T} = \mathbf{m}\times\mathbf{B} = |\mathbf{m}||\mathbf{B}|\sin\theta \tag{4}$$

In eq 4, θ is the angle between $\mathbf{m}$ and $\mathbf{B}$, and sin θ reaches maximum when $\mathbf{m}$ and $\mathbf{B}$ are perpendicular to each other and reaches minimum when $\mathbf{m}$ and $\mathbf{B}$ are aligned. Based on eq 4, a magnetic particle aligns the direction of its magnetic moment to the direction of the magnetic field. To increase the magnetic torque on the particle, a large field strength is required, and magnetic particles made from permanent magnet are used.

When multiple magnetic particles are present in the workspace, the magnetic particles form an aggregate due to interparticle magnetic force. Assuming the aggregate formed is symmetrical and the particles have the same size and are of the same material, the magnetic torque generated on the magnetic aggregate is[45]

https://dx.doi.org/10.1021/acsnano.0c00959
ACS Nano 2020, 14, 3805−3821

$$\mathbf{T} = \frac{3\mu_0 \mathbf{m}^2}{4\pi}\sin(2\theta)\sum_{i=1}^{N/2} 2r_i \sum_{\substack{j=-\frac{N}{2} \\ j\neq i}}^{N/2} \frac{1}{r_{ij}^4} \quad (5)$$

where N is the number of particles in the aggregate, r_i is the distance between the i-th particle and the center of the aggregate, and r_{ij} is the distance between the centers of mass of i-th particle and that of j-th particle. The magnetic torque of the magnetic aggregate increases when its size increases.

Magnetic Particle Dynamics. When a magnetic particle is introduced into cell medium or the intracellular environment, upon the exposure to a magnetic-field gradient, the freely moving particle subjects to a magnetic force, fluidic drag force, buoyant force, gravitational force, and a thermal force that induces Brownian motion.[46] The particle dynamics is

$$\mathbf{F}_{\text{magnetic}} + \mathbf{F}_{\text{thermal}} + \mathbf{F}_{\text{buoyant}} + \mathbf{F}_{\text{gravitational}} = m\ddot{\mathbf{P}} + 6\pi\eta r\dot{\mathbf{P}} \quad (6)$$

where $\mathbf{F}_{\text{magnetic}}$ is the random thermal force and $\mathbf{P}$ is the particle position in 3D. The buoyant force $\mathbf{F}_{\text{buoyant}}$, the gravitational force $\mathbf{F}_{\text{gravitational}}$, and the inertia of the particle $m\ddot{\mathbf{P}}$ are negligible due to the particle's small mass.[22] The thermal force on the magnetic particle $\mathbf{F}_{\text{thermal}}$ depends on the size and the environmental temperature. Considering the small mass and the small inertia of the particles of a few microns or lower, particle dynamics becomes[22]

$$\mathbf{F}_{\text{magnetic}} + \mathbf{F}_{\text{thermal}} = 6\pi\eta r\dot{\mathbf{P}} \quad (7)$$

Actuation of Magnetic Particles. Due to the convenience of generating a magnetic gradient force on magnetic particles, direct force application is often used for cellular and intracellular stimulation. Within a magnetic gradient field, magnetic particles are subjected to a magnetic force that can be controlled by controlling the distance between permanent magnets and the particles or by controlling the current applied to electromagnetic coils (Figure 1a). Permanent magnets generate a large magnetic field without generating heat in the workspace, and the generated field depends on the shape, material, and lifetime of the permanent magnets. Compared with permanent magnetic systems, an electromagnetic system is programmed to generate more complex field profiles (*e.g.*, rotating magnetic field and time-variant magnetic field) and fast dynamics by controlling the current applied to the electromagnetic coils in the system. The controllable force exerted on the magnetic particles can be used for measuring the mechanical properties by relating the applied force and the resulting cellular structural deformation and for studying the mechanotransduction of cellular structures by force stimulation.

A rotating magnetic field actuates a magnetic particle or a magnetic rod to rotate around its center axis to exert a torque on the cellular structure to be measured (Figure 1b). When subjected to a magnetic field, the magnetic particle or rod aligns its magnetic moment with the magnetic-field direction. Helmholtz coils are the most commonly used due to their capability of generating a rotatory magnetic field with uniform magnetic-field strength in a workspace as large as several centimeters.[47] Rotating permanent magnets are also used to generate a rotatory magnetic field with low heat generation than electromagnetic coils; however, the mechanical rotation of the permanent magnets cannot generate high-frequency rotation of the field (*e.g.*, >100 Hz), and the strength of the

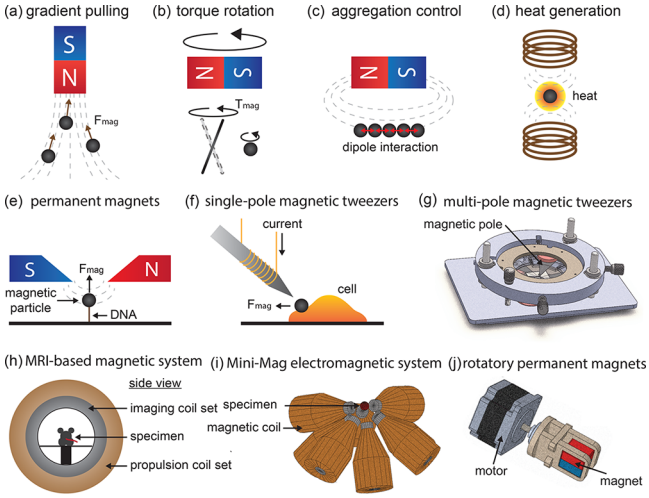

Figure 1. (a–d) Principles of magnetic micromanipulation and representative magnetic micromanipulation systems. (a) Magnetic gradient pulling. Magnetic particles subject to a magnetic force generated by magnetic gradient. It is used to apply a direct force on a magnetic particle that is attached to a cell structure/structure. (b) Magnetic torque rotation. Magnetic particles rotate and exert a torque to deform a structure to which magnetic particles are attached. (c) Magnetic aggregation control. Magnetic particles assemble into an aggregate due to dipole interactions. (d) Magnetic heat generation. Magnetic particles are controlled to generate heat from the induced current generated by a high-frequency alternating magnetic field. (e–j) Representative magnetic micromanipulation systems using permanent magnets or electromagnetic coils, including magnetic tweezers using a permanent magnet (e), single-pole magnetic tweezers (f), multi-pole magnetic tweezers (g), MRI-based magnetic system (h), Mini-Mag electromagnetic system (i), and rotatory permanent magnetic system (j). Detailed comparisons of these magnetic-field generation systems are summarized in Table 1. (g) Adapted with permission from ref 22. Copyright 2019 AAAS. (i) Adapted with permission from ref 29. Copyright 2013 IEEE. (j) Adapted with permission from ref 28. Copyright 2017 IEEE.

torque is difficult to be precisely controlled due to the inhomogeneity of different permanent magnets. Exerting magnetic torque for measurement and stimulation has been used for characterizing the mechanotransduction signaling pathways both on cell surface and inside the cell[48] and for intracellular navigation of helical swimmers.[49]

In the aggregation of magnetic particles (Figure 1c), magnetic particles within the workspace are magnetized by the magnetic field and subsequently generate an attractive force among neighboring particles. An aggregation of magnetic particles was used to mimic biochemical molecular clustering effects, when conformational clustering of agglomerate receptors triggers receptor-mediated signal transduction.[50] The interparticle force is determined by the magnetic-field strength and the particle-to-particle distance.[51] Since the interparticle force is relatively small (picoNewton)[52] due to the small volume of the particles, a large magnetic-field strength is usually used in order to generate sufficient forces to form aggregates.

Magnetic heating of ferromagnetic particles (Figure 1d), or magnetic hyperthermia, has been used to generate heat for studying cell signaling after heat stimulation[53] and for the use of hyperthermia as a cancer treatment approach complementary to chemotherapy and radiotherapy.[54,55] It has been shown

https://dx.doi.org/10.1021/acsnano.0c00959
ACS Nano 2020, 14, 3805–3821

that alternating magnetic fields at frequencies between 300 kHz and 1 MHz can efficiently generate an alternating current on microscale magnetic particles and thus generate heat to the cellular structures or the microenvironment surrounding the magnetic particles.[56] The locally generated heat from the alternating magnetic field can be used to stimulate cellular or intracellular structures and trigger cell apoptosis.

Heat is generated when energy from an alternating magnetic field is delivered to magnetic nanoparticles. The heat generation mechanisms can be categorized into hysteresis heating, Eddy current heating, Brownian relaxation, and Néel relaxation.[56,57] When a magnetic field is applied to ferromagnetic materials such as iron, the atomic dipoles align themselves with the external field during magnetization. Under an alternating magnetic field, the magnetization and demagnetization cycles lead to the cyclic change of the atomic dipole directions, and the energy difference between the magnetization process and the demagnetization process (*i.e.*, enclosed area in the $B-H$ curve) is the heat dissipated during one cycle.[57] However, since magnetic nanoparticles usually exhibit paramagnetic and superparamagnetic properties with small hysteresis, hysteresis heating is negligible compared to the Néel and Brownian relaxations.[58] Eddy current is the electric current generated by an alternating magnetic field, and its power density equals $Ef^2H_{max}d^2$, where E is the Eddy current coefficient, f is the frequency of the alternating magnetic field, H_{max} is the maximum flux density, d is the diameter of the nanoparticle. Since the size of nanoparticles is smaller than 100 nm, the Eddy current generated at this scale is usually insignificant.[57]

Néel relaxation occurs because magnetic dipoles are more energetically favorable to be aligned with the crystal planes in a material. An alternating magnetic field rapidly changes the dipoles' alignment toward the crystal planes, which generates heat.[58] Meanwhile, in a low-viscosity liquid, a particle physically rotates under an alternating magnetic field to align the magnetic moment direction to the direction of the external magnetic field. The induced rotation leads to frictional heating of the surrounding medium, referred to as Brownian relaxation.[59] Néel and Brownian relaxations were shown to be the dominant mechanism for heat generation in nanoparticle hyperthermia. Néel relaxation alone is the dominant mechanism when particles are bound to target structures such as *via* antibodies.[58,59]

Magnetic-Field Generation Systems. The motion of magnetic particles within a magnetic field was used to measure the rheological properties of fluidic medium in the 1920s.[29] In 1949, Francis Crick and Arthur Hughes demonstrated the use of an external magnetic field to manipulate magnetic particles cultured with cells and tissues.[60] Although the method was self-admittedly crude due to the insufficiency in calibration and field control, the technique was used for many years in the studies of cytoplasm rheology and mechanical properties of cells.[60] In 1996, Allemand *et al.* used permanent magnets with sharp tips to exert forces on magnetic particles attached to DNA for studying the force needed to unfold DNA by taking advantage of the high force output of permanent magnets (Figure 1e).[61] However, force control of a permanent magnet system relies on the control of the magnet's positions, and force modeling is complicated as the force output changes with the material type, lifetime, and the shape of the magnets. To overcome these difficulties, Fischer *et al.* formed an electromagnetic coil on a ferromagnetic core with a sharp tip (Figure 1f).[62] When the current is applied to the magnetic coil, a high magnetic-field gradient is generated near the sharp tip of the magnetic pole, generating a controllable force on the magnetic particle attached to the structure of interest (*e.g.*, integrin on the cell membrane). The single-pole magnetic tweezers only apply one-directional attractive forces and cannot be used to control a freely moving particle.

In 2005, de Vries *et al.* developed multipole (quadrupole, hexapole) magnetic tweezers for applying forces on a magnetic particle in different directions.[63] With the capability of navigating a freely moving particle, the multipole magnetic tweezers enabled the measurement of intracellular viscosity. However, particle navigation was controlled in an open-loop manner since the small inertia and fast dynamics of magnetic microparticles pose difficulties for position control; and force application was through empirically applying current to each of the coil in turn without the guidance from a force model. Zhang *et al.* developed a model for multipole magnetic tweezers control by assuming each of the magnetic pole as a magnetic monopole.[36] By relating normalized current and particle position, accurate 3D particle positioning was achieved. Wang *et al.* further related magnetic force to electric current applied to each magnetic coil and the particle position within the workspace[15] and achieved controlling particle position and force inside a single cell (Figure 1g).[16]

In addition to magnetic tweezers, other electromagnetic systems, including MRI-based system,[32] OctoMag,[30] and MiniMag[29] and DeltaMag,[31] have also been developed to generate magnetic gradient through controlling the current in each coil (Figure 1h,i, and Table 1). In comparison, permanent magnetic systems have the advantages of low heat generation and strong field strength, in which the position and/or direction of the permanent magnets can be controlled to create an inhomogeneous magnetic-field flux, thus a magnetic gradient. For instance, a rotatory permanent magnet system was designed to control the moment direction of eight permanent magnets to create a controllable magnetic gradient field up to 2 T/m (Figure 1j).[28] With gradient-generated forces, devices in the size of centimeters to submillimeters were actuated to perform imaging, biopsy, and surgery inside organs (*e.g.*, stomach, ear, and eye),[64] function as controllable valves in microfluidic channels,[65] and navigate inside a mouse embryo for measurement.[15]

Magnetic Measurement of Cellular and Intracellular Structures. The response of a cell and intracellular structures to mechanical forces can be viscous, elastic, or viscoelastic. When subjected to a magnetic field, a magnetic particle can be controlled to apply a controllable force to a cellular or intracellular structure (Figure 2a). By relating produced deformation caused by the magnetic force *via* mechanics models, the mechanical properties of cell and organelles (*e.g.*, endoplasmic reticulum, nucleus, *etc.*) can be characterized, providing an untethered means for characterizing mechanical properties of cell and intracellular structures.

Cell Mechanics Measurement. To measure the mechanical properties of a cell, the magnetic particle attached on the cell (*e.g.*, integrin-antibody-coated magnetic particles attached on integrin of cell surface) is controlled to apply a force or torque on the cell by controlling an external magnetic field.[65,68] Under mechanical loading, cells undergo viscoelastic deformations. Based on the force-deformation relationship (termed as creep response), the elasticity and viscosity of the cell are quantified. For instance, Bausch *et al.* characterized the

https://dx.doi.org/10.1021/acsnano.0c00959
ACS Nano 2020, 14, 3805−3821

Table 1. Representative Magnetic Micromanipulation Systems

systems	rotatory permanent magnets	MiniMag	DeltaMag	MRI-based	multipole magnetic tweezers
actuation method	magnetic gradient pulling	magnetic gradient pulling	magnetic torque	magnetic gradient pulling	magnetic gradient pulling
setup	eight permanent magnets mounted on rotatory motors	eight electro-magnetic coils	three mobile electromagnetic coils and three motors	MRI scanner; electromagnetic coils	magnetic poles on electromagnetic coils
actuation field	∇B_{max} = 0.9 T/m	∇B_{max} = 5 T/m	B_{max} = 23 mT	∇B_{max} = 0.4 T/m	∇B_{max} = 50 T/m
advantages	no heat generation compared to electromagnets; multiple locomotion methods	multiple locomotion methods (*e.g.*, rotating, gradient pulling, and stick–slip)	larger effective workspace systems with stationary coils	availability of simultaneous deep-body image feedback; closed-loop control	high gradient produced at sharp tips
limitations	low-frequency field modulation; field cannot be turned off	field is limited by the size, resistance, and heat generation of coil wires	calculation of magnetic field is not straightforward	combining MRI-based actuation and sensing is challenging	misalignment of poles can cause unbalanced forces
references	28	29, 30	31	32–35	21, 36

viscoelastic properties of cells by applying pulling forces on the cell through a ferromagnetic particle (4.5 μm in diameter) using single-pole magnetic tweezers.[66,69]

Cell plasticity was measured by the irreversible deformation on the cell after force application on the cell surface using a 4 μm magnetic particle (Figure 2b).[70] Magnetic measurement was also extended to long-term cell characterization during cell migration, cell mitosis, cancer progressions, and stem cell maturations. For instance, Osborne *et al.* characterized the stiffness changes of cells during TGF-β-induced EMT (epithelial-to-mesenchymal transition) over time and revealed a functional connection between attenuated cell stiffness, stiffening response, and the increment of invasion capacity during epithelial-to-mesenchymal transition.[71]

Cytoplasm Viscosity Measurement. Cytoplasm of living cells is a complex system where many metabolic reactions take place.[72] The aqueous compartment of cytoplasm consists of a complex array of organized macromolecular structures, including skeletal elements and organelles (*e.g.*, ions, amino acids) and dissolved small and large solutes (*e.g.*, proteins). Cytoplasm viscosity, defined as viscosity sensed by a small probe which does not directly interact with intracellular structures,[73] is important for describing the status of cellular cytoskeleton and helps to understand intracellular transport. Using magnetic micromanipulation techniques, cytoplasm viscosity can be measured through moving a magnetic particle inside the cell (Figure 2c) and then calculated by the Navier–Stokes equation[74] and through rotating a magnetic wire/rod inside a cell and calculated through fitting the magnetic torque and rotation speed into viscoelastic mechanical models.[75] Bausch *et al.* navigated a single 1.3 μm magnetic particle in a macrophage to measure the viscoelasticity of the cell's cytoplasm by tracking the particle's moving speed under a constant force application. The result showed that viscosity of the cell's cytoplasm was 2–7 mPa·s.[66] Berret *et al.* controlled the rotation of magnetic wires inside a cell to measure the rheological properties of the cytoplasm.[75] Unlike the translational movement of magnetic particles inside a cell, which only measures the cytoplasm viscosity, the rotating wire can differentiate liquid-like (*i.e.*, viscosity) from gel-like (*i.e.*, viscoelasticity) behaviors by observing the transient frequency between a synchronous and an asynchronous regime of rotation.[75]

Cell Nucleus Measurement. The cell nucleus is the largest organelle inside the eukaryotic cell. Altered mechanical properties of the cell nucleus are known to be related to diseases such as Hutchinson–Gilford syndrome,[76] cardiomyopathy,[77] and cancers.[15] Measurements of cell nuclear mechanics have been performed using atomic force microscopy[78] and micropipette aspiration[79] on isolated nuclei, which were isolated from intact cells either mechanically or chemically. Untethered techniques enable measurement of cell nuclei in intact cells. Among untethered techniques, optical manipulation only generates forces around 10 pN, which is insufficient to deform the cell nucleus with observable deformations.

Magnetic tweezers (single-pole and multipole devices) have been used to create a controllable magnetic field to apply a known force on magnetic bead attached to the cell nuclear envelope. Relating the deformation and the applied force through mechanics models, the mechanical property of the cell nuclei can be measured. By attaching an antibody-coated magnetic particle onto Nesprin (a nuclear envelope protein)

https://dx.doi.org/10.1021/acsnano.0c00959
ACS Nano 2020, 14, 3805–3821

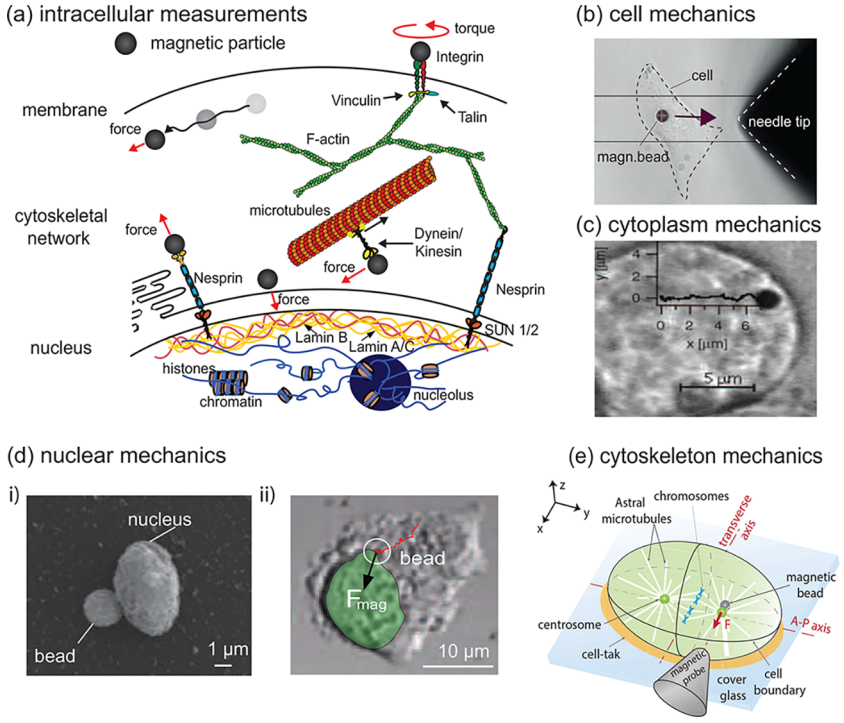

Figure 2. (a) Mechanical measurement on cell surface, cytoplasm, cell nucleus, cytoskeleton, and intracellular motors, using magnetic controlled particles. Reproduced with permission from ref 15. Copyright 2018 Company of Biologists. (b) Cell mechanics measurement through stretching a magnetic particle attached to cell surface. Reproduced with permission from ref 70. Copyright 2016 Springer Nature. (c) Cytoplasm viscosity measurement through tracking the speed of magnetic particle moved in cytoplasm. Adapted with permission from ref 66. Copyright 1999 Elsevier. (d) (i) Nuclear stiffness measurement through applying an oscillation force on an isolated nucleus. Reproduced with permission from ref 67. Copyright 2014 Springer Nature. (ii) Intracellular magnetic particle navigation and cell nucleus mechanical measurement. Adapted with permission from ref 22. Copyright 2019 AAAS. (e) Measurement of forces for a cell to maintain the position and orientation of spindle during cell division. Reproduced with permission from ref 3. Copyright 2016 AAAS.

and applying an oscillating force (35 pN) on cell nucleus, Guilluy *et al.* found that mechanotransduction exists on the nuclear envelope (Figure 2d).[67] Wang *et al.* developed a multipole magnetic tweezers device and controlled a 0.7 μm magnetic particle to measure the cell nuclear mechanics inside an intact cell (Figure 2d).[22] Measurement was made on different locations of the nuclear envelope, and the polarity of the nuclear mechanics in migrating cells was discovered. Subramaniam *et al.* microinjected a single 1 μm magnetic particle into the nucleus of a living cell and measured the viscoelasticity within the cell nucleus.[80]

Measurement of Other Intracellular Structures. Through applying a controllable force or torque to balance the active force produced by the motor protein in the cytoplasm, magnetic actuation was used to quantify the driving force/torque of an isolated motor protein, such as kinesin, dynein, and rotary motor protein.[81,82]

Mechanical measurements were also made on the cytoskeleton for understanding how the molecular forces applied on the cytoskeleton affect cell mitosis and cell migration. Garzon-Coralin *et al.* measured the forces required by a cell to maintain the position and orientation of the mitotic spindle during cell division (Figure 2e).[3] To measure mitotic forces *in vivo*, a 1.0 μm superparamagnetic particle was injected into a *Caenorhabditis elegans* embryo, and single-pole magnetic tweezers were used to exert forces up to 200 pN to the mitotic spindles. To further increase force output for manipulating the cytoskeleton, Tanimoto *et al.* built a single-pole magnetic tweezers with strong neodymium super magnets, capable of applying forces up to 1.5 nN to move microtubule asters in a fertilized sea urchin egg.[83] With the ability to slow down and move the asters centering motion, they measured the force associated with the migration and centering of the aster and estimated the number of motor proteins involved in the process.

In addition to cytoskeleton, DNA strands were measured using magnetic micromanipulation. Measuring the mechanical force required to stretch or twist DNA molecules was conducted to study the stability of DNA structures and the mechanics of DNA polymerization.[75] Through mechanical stretching or twisting DNA strands using magnetic particles attached to one end of the DNA strand while fixing the other end onto the substrate, the force needed for unwinding or rezipping DNA, the molecular force in DNA replication, and the force on torsional constraints were measured.[75] Furthermore, Ebright *et al.* developed a single DNA-nanomanipulation approach using magnetic field for studying the extension of one turn of DNA by RNA polymerase.[84]

Magnetic Stimulation of Cellular and Intracellular Structures. Applying mechanical stimulation on cellular structures and studying downstream effects are necessary for deciphering how cells adapt to the mechanical-force/shear-abundant microenvironment, how cancer cells pass through a tight space *in vivo*, and how targeted stimulation on cellular structures can offer other therapeutic approaches. Taking advantage of the capabilities of generating well-controlled force, torque, and heat on magnetic particles through controlling the magnetic field, magnetic micromanipulation is

https://dx.doi.org/10.1021/acsnano.0c00959
ACS Nano 2020, 14, 3805−3821

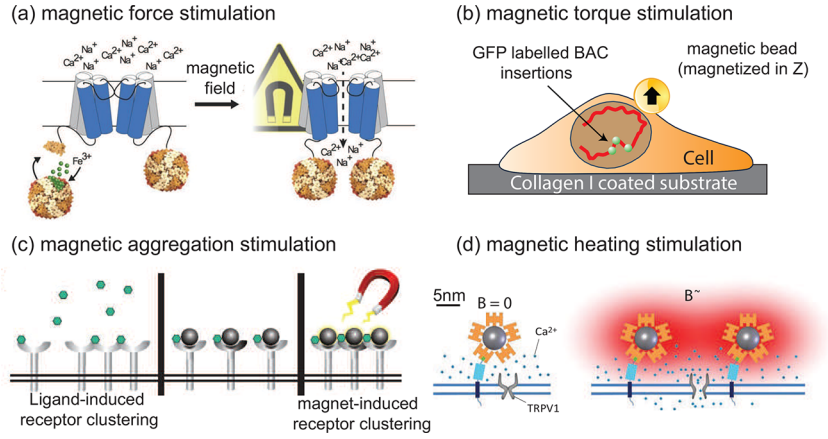

Figure 3. Different types of magnetic stimulation. (a) Ferritin is genetically fused with TRPV4 cation channel. Upon magnetic-field actuation, TRPV4 is stretched by magnetic force, resulting in calcium influx. Adapted with permission from ref 85. Copyright 2016 Springer Nature. (b) Magnetic nanoparticle is bound to integrin through coating. Upon activation of magnetic field, the particle rotates and applies torque on integrin, resulting in stress propagation to chromatin and transcription upregulation. Adapted with permission from ref 40. Copyright 2016 Springer Nature. (c) Magnetic particles are bound to FcεRI receptors individually. Magnetic particles are magnetized and experience interparticle attractive force with exposure to a magnetic field, resulting in receptor clustering and signal transduction. Adapted with permission from ref 86. Copyright 2008 Springer Nature. (d) Magnetic particles are used to execute thermal activation of TRPV1 by exposing magnetic particles in a high-frequency alternating magnetic field. Adapted with permission from ref 87. Copyright 2010 Springer Nature.

a powerful technique for stimulating cellular and intracellular structures.[10]

Magnetic Force for Cellular and Intracellular Stimulation. Due to the convenience of generating a magnetic gradient force on magnetic particles, direct force application is the most commonly used method in cellular and intracellular stimulation. As shown in eq 1, the magnetic force on a particle depends on the gradient of the magnetic field. The force on the particle is then controlled by controlling the magnetic-field gradient through controlling the distance between permanent magnets and the magnetic particles or by controlling the electric current applied to the electromagnetic coils. The particles, coated with antibodies to facilitate binding to specific cellular structures for studying mechanosensitive ion channels/receptors and intracellular organelles, are controlled to apply forces on the cell membrane and intracellular structures.

Cell membrane is abundant with mechanical-sensitive receptors and ion channels, such as integrin receptor,[85] cadherin adhesion molecule,[88] ErbB receptor,[89] frizzled receptor,[90] notch receptor,[88] TREK-1 channel,[91] TRPV4 channel,[85] *etc.* Taken as an example, integrin is a mechanosensitive protein transmitting forces from the extracellular matrix to the cytoskeleton.[40,85] By exerting a magnetic force on integrin through magnetic particles, force transmission of integrin from extracellular environment to the intracellular environment and its downstream biochemical signaling pathways are studied. In ref 92, fibronectin-coated magnetic particles were used to apply a magnetic force of 1 nN on integrin, resulting in the reinforcement of focal adhesion of cells. For mechanosensitive ion channels, transient receptor potential cation channel protein TRPV4 was fused with ferritin (iron storage protein) to generate magnetic forces on TRPV4 when subjected to a magnetic field.[85] With a magnetic force applied on ferritin, the state change of the ion channel was triggered from "close" to "open", and calcium influx controlled by the channel increased (Figure 3a). By remotely controlling the magnetic field, the activation of the ion channel and the calcium influx was rapidly and reversibly controlled, which was used for regulating neural circuits' dynamics.

The response of intracellular structures and organelles to applied magnetic force stimulation was also investigated. Through applying magnetic forces on the microtubule, Hoffmann *et al.* studied the effect of localization forces on microtubule nucleation and assembly.[92] They observed that microtubules assemble into an asymmetric array of polarized fibers and the orientation was dictated by the direction of magnetic forces. Wang *et al.* introduced a magnetic particle into a cell through endocytosis and applied a magnetic force repeatedly on the same location on the nuclear envelope. It was shown that the local Young's modulus of the cell nucleus increases due to stiffening,[22] due to the remodeling and reinforcement of the lamin network underneath the nuclear envelope under mechanical stimulation.

Magnetic Torque for Cellular and Intracellular Stimulation. Magnetic torque aligns the magnetic moment direction to the direction of the magnetic field. When subjected to a rotating magnetic field, a magnetic rod or tube (magnetic moment in the direction of the long axis) or a paramagnetic particle (with defined magnetic moment) rotates with the magnetic field, generating a torque on the structure the rod/tube/particle is attached to. After coated with adhesion molecules or antibodies to tightly bond onto the cellular structure to stimulate, functionalized paramagnetic particles can be used to stimulate targeted cellular structures. For instance, to target the mechanoreceptor integrin, magnetic particles can be coated with either Arg-Gly-Asp (RGD) or poly-L-lysine (PLL) to form tight adhesions between integrin and the cell surface. When applying a rotating magnetic field, the magnetic particles apply a torque on integrin (Figure 3b). Using this approach, Wang *et al.* showed that integrin B1 functions as a mechanoreceptor on the cell membrane and transmits the mechanical torque exerted on the cell membrane to the cytoskeleton.[93] This approach was also used to reveal that local stresses applied to integrin propagate from the cell membrane to the actin cytoskeleton and then to the LINC and

https://dx.doi.org/10.1021/acsnano.0c00959
ACS Nano 2020, 14, 3805−3821

Table 2. Magnetic Measurement of Cellular and Intracellular Structures

measurement target	technique	system description	magnetic particle	force/torque
cell membrane viscoelasticity[69]	gradient pulling	single-pole magnetic tweezers	4.5 μm paramagnetic particles were fixed to the integrin receptors of the cell membrane	500−2500 pN forces pulse (1 s) was applied on the particles
cell membrane elasticity[156]	twisting torque	3D magnetic twisting cytometry	4.5 μm ferromagnetic particles were attached to cell membrane and twisted by a twisting field to induce a local stress on the cell membrane	local stress of 45 Pa with frequency of 0.83 Hz on the cell membrane
cell membrane elasticity[65]	twisting torque	3D magnetic twisting cytometry	4 μm ferromagnetic particles were attached to cell membrane and twisted by a twisting field to induce a local stress on the cell membrane	local stress of 15 Pa with frequency of 0.1 Hz on the cell membrane
cell membrane viscoelasticity[68]	twisting torque	magnetic twisting cytometry (one pair of coils)	4.5 μm ferromagnetic particles coated with Arg-Gly-Asp (RGD) peptide were attached to cell membrane and twisted by a twisting field to induce a local stress on the cell membrane	local stress of 17.5 Pa with frequency of 0.3 Hz on the cell membrane
cell membrane viscoelasticity and stiffening[71]	gradient pulling	UNC 3D force microscope (two-layer multipole magnetic system)	4.5 μm paramagnetic particles coated with fibronectin were attached to cell membrane and pulled by magnetic force to determine the effect of EMT on cell stiffness and stiffening response	50 pN of force pulse for 5 s, followed by a relaxation of 10 s was applied to fibronectin-coated magnetic particles
cell membrane plasticity[70]	gradient pulling	single-pole magnetic tweezers	5 μm superparamagnetic particles were attached to cell membrane	10 nN force (duration 3 s) in alternating directions was applied on the cell surface
isolated nucleus membrane stiffening[67]	gradient pulling	UNC 3D force microscope (two-layer multipole magnetic system)	2.8 μm particle coated with anti-Nesprin-1 antibody was attached to the isolated nucleus	35 pN oscillating forces were applied on the magnetic particles
nucleus membrane stiffness[22]	gradient pulling (indenting)	multipole magnetic tweezers	0.7 μm magnetic particle was internalized into cell and manipulated *via* magnetic gradient to indent different positions on nucleus	force up to 60 pN with a resolution of 4 pN for a period longer than 30 min was applied on the magnetic particles
chromatin in nucleus viscoelasticity[80]	gradient pulling	multipole magnetic tweezers	a single 1 μm magnetic particle was inside nucleus	force of 110 pN was applied on the particle
cell cytoplasm viscoelasticity and active force[66]	gradient pulling	single-pole magnetic tweezers	1.3 μm superparamagnetic particles were internalized by macrophages	Force of 50−900 pN was applied
cell cytoplasm viscoelasticity[75]	torque rotating	multipole magnetic tweezer (four poles) to generate rotating magnetic field	magnetic wires (1.9−5.9 μm) were fabricated by γ-Fe_2O_3-coated particles and oppositely charged polyelectrolytes	magnetic wires with length of 2−6 μm were exposed under a 14 mT rotating field with frequency ranging from 0 to 160 Hz
isolated DNA molecule[84]	gradient and torque	a pair of permanent magnets	DNA was torsionally constrained and mechanically stretched by application of a pair of magnets above the DNA	paramagnetic particle was attached at one end of the DNA molecule with another end attached to the glass substrate
isolated kinesin[82]	gradient pulling	spatially uniform magnetic-field gradient	superparamagnetic particle (2.8 μm) was attached to the positive end of an isolated microtubule bounded with multiple kinesin on the substrate	force ranging from 0 to 31 pN was applied by the particles
bacterial flagellar motor[81]	torque	a pair of permanent magnets; a superparamagnetic particle attached to flagellar	1.0 μm magnetic bead lined to bacterial flagellar motor was used to manipulate the external load on the motor by adjusting the magnetic field	torque was applied by rotating a pair of magnets above to stall the motor
mitotic spindles[3]	gradient pulling	single-pole magnetic tweezers	1.0 μm superparamagnetic particle was injected into the cell (embryo)	force of 200 pN was applied to mitotic spindles
aster in egg[83]	gradient pulling	single-pole magnetic tweezers with permanent magnet	particles with size of 2.8 μm or 200−800 nm were injected into the egg	magnetic particles rapidly aggregated and bound to the aster center allowed direct force application on the asters with force up to 1500 pN

https://dx.doi.org/10.1021/acsnano.0c00959
ACS Nano 2020, 14, 3805−3821

through lamina-chromatin interactions, stretched chromatin, and upregulated transcription.[93]

Recently, rotating or oscillating magnetic particles inside a cell were found to be capable of triggering cell apoptosis and potentially be used for cancer treatment.[94−98] After cancer cells internalize magnetic particles through endocytosis, magnetic particles were found to be present inside the lysosomes, an organelle responsible for intracellular transportation. When a rotating magnetic field was applied, the rotation of the magnetic particles caused lysosomal membrane lysis and the leakage of hydrolases, which degraded most of the cellular macromolecules and caused cell apoptosis.[97] To increase the efficacy of trigging cancer cell death *in vitro* by applying magnetic torques, magnetic particles were coated with antibodies to specifically target lysosomes inside the cells. Zhang *et al.* used magnetic particles coated with LAMP1 antibody (lysosomal-associated membrane protein 1) to enhance the cellular internalization through lysosomes.[99] Rat insulinoma tumor cells and human pancreatic β cells were found to undergo apoptosis after the rotation of magnetic particles inside the cells.

Magnetic Aggregation Control for Cell Stimulation. When subjected to a magnetic field, ferromagnetic particles are magnetized, generating an attractive force among neighboring particles and forming aggregations. Mannix *et al.* conjugated magnetic particles with antibodies to target the FcεRI receptors (Figure 3c).[86] Without a magnetic field, magnetic particles bound to individual receptors, and no downstream signaling pathways were activated. Upon magnetic-field application, the magnetic particles were magnetized and formed aggregates, triggering FcεRI receptor oligomerization and downstream calcium signaling. Similarly, Cho *et al.* used magnetic particles conjugated with antibodies to aggregate death receptor 4.[52] When a magnetic field was applied, caspase-3, the effector caspase and death signal, was observed upon the aggregation of death receptor 4, causing apoptosis of DLD-1 colon cancer cells *in vitro* and morphological changes in zebrafish *in vivo*.

In addition to mimicking the conformation aggregation of receptors, the aggregation of functionalized magnetic particles can locally enrich the particles to activate cell signaling pathways. Etoc *et al.* reported that the accumulation of functionalized magnetic particles activated Rac-GTPase signaling pathways that locally remodeled the actin cytoskeleton and led to morphological changes in a living cell.[100] The results demonstrated that magnetic particles can be used to control local cell signaling and morphological changes through magnetically controlling the localization of particles.

Heat Generation by Alternating Magnetic Field for Cell Stimulation. An alternating magnetic field induces an electrical current on magnetic particles and generates heat. Hence, magnetic micromanipulation provides a means to control heat generation in target cells or tissue. When magnetic particles are bound on the cell surface receptor or deposited within tissue, the magnetically generated heat is dissipated and causes temperature increase locally. This capability of wirelessly controlling temperature has been used to remotely control the activation of temperature-sensitive ion channels and trigger hyperthermia for cancer treatment. Transient receptor potential vanilloid 1 (TRPV1), a cation channel known to be temperature-sensitive with a threshold of 42 °C,[87] was targeted to trigger specific signaling pathways by magnetic heating[33] (Figure 3d). Huang *et al.* found that thermal activation of TRPV1 conjugated with magnetic particles increased the intracellular calcium concentration of human embryonic kidney HEK 293 cells, increased action potential in hippocampal neuron, and triggered responses in *C. elegans*.[87] Stanley *et al.* used iron oxide particles coated with antibodies targeting TRPV1 to locally activate TRPV1 by applying an alternating magnetic field.[101−103] When the local temperature rose, TRPV1 gated calcium to stimulate the INS insulin gene, and insulin release was increased and blood glucose was lowered in mice.

When temperature rises in the microenvironment, the apoptosis of cancer cells occurs earlier than in normal cells.[104,105] Using remote temperature control with the application of an alternating magnetic field on magnetic particles, several studies explored hyperthermia treatment of cancer cells.[106−109] Gordon *et al.* reported hyperthermia treatment and observed that the hyperthermia-treated cancer cells exhibited condensed cytoplasm and condensed pyknotic nuclei, while the surrounding normal cells were mostly physiologically intact.[110] Jordan *et al.* described a method known as magnetic fluid hyperthermia by using an alternating magnetic field and a ferrofluid consisting of dextran-coated magnetic particles to treat WiDr human colon adenocarcinoma.[94] Compared with traditional cancer therapies such as chemotherapy and radiotherapy in which cancer cells are targeted for their fast DNA replication capability, magnetically controlled hyperthermia can potentially circumvent tumor resistance caused by gene mutations.[111]

SUMMARY AND OUTLOOK

Magnetic Measurement and Stimulation. The development of magnetic micromanipulation systems, using electromagnets or permanent magnets, has enabled a multitude of applications for cellular and intracellular measurement and stimulation. Different configurations of magnetic-field generation systems were developed to control a magnetic particle or particles to apply a force on cellular/intracellular structures for measurement or stimulation. Magnetic particles have been controlled by an external magnetic field to exert forces/torques and perform mechanical measurements on the cell membrane, cytoplasm, cytoskeleton, nucleus, intracellular motors, *etc.* (see Table 2). They have also been used to generate aggregations to trigger cell signaling pathways and produce heat to cause cancer cell apoptosis for hyperthermia treatment (see Table 3). Magnetic micromanipulation has become an important tool in the repertoire of toolsets for cell measurement and stimulation and will continue to be used widely for further explorations of cellular/intracellular structures and their functions. Integration of the magnetic micromanipulation with other technologies such as microfluidics would enable time-lapsed measurement and stimulation during cell/tissue growth, embryo development, and stem cell differentiation, to name just a few.

Magnetic micromanipulation and stimulation on cellular structures also promise therapeutic approaches. As illustrated in Figure 4a, mechanical stimulation of cell apoptosis receptors can trigger cell apoptosis pathways;[97] mechanical ablation of cellular structures *via* force or torque application can cause cell death;[96] and magnetically delivery of heat for hyperthermia can effectively raise temperature for tumor treatment.[86] It has been shown that when magnetic field was applied, caspase-3, the effector caspase and death signal, was observed upon the aggregation of death receptor 4, causing cell apoptosis. Other cell death-related receptors, such as FcεRI,[116] PD-1,[117] and

https://dx.doi.org/10.1021/acsnano.0c00959
ACS Nano 2020, 14, 3805−3821

Table 3. Magnetic Stimulation of Cellular and Intracellular Structures

stimulation target	technique	system description	magnetic material	parameters
integrin of mouse embryonic fibroblast[157]	force control	magnetic tweezers	3 μm fibronectin-coated particle	1 nN on integrin to study the role of α-actinin in force transmission
TRPV4 cation channel in HEK 293 cells, zebrafish (Danio rerio) larvae, and Drd1a::Cre mice[85]	force control	Magneto2.0	TRPV4 was fused with ferritin and became magnetically sensitive	both *in vitro* and *in vivo*, TRPV4 were triggered, and neurons signaling were controlled in a field of 50 mT and 500 mT
ErbB receptor of MCF7 cells[89]	force and heating control	magnetic tweezers	254 nm diameter and 88.7 nm length Fe−Au nanorods were coated with polyethylene glycol and heregulin, a ligand of ErbB receptor	magnetic tweezer was applied with 1 A to apply a force of 4.1 pN on nanorods; alternating magnetic field (50−250 kHz, 1.3−6.5 A/m) was tested on Fe−Au nanorods to show hyperthermia of breast cancer cells
frizzled receptor of human mesenchymal stem cells[90]	force control	commercial oscillating magnetic bioreactor MICA	337 nm magnetic particles were functionalized with anti-frizzled	commercial oscillating magnetic bioreactor MICA was used to apply a field of 25−120 mT for 1 or 3 h at around 1 Hz; frizzled receptor was proven to be mechanosensitive
TREK-1 channel on human bone marrow stromal cells (HBMSC)[91]	force control	permanent magnet up and down at 1 hz	250 nm magnetic particles were coated with either anti-TREK-1 antibody or RGD	HBMSC was stimulated by a force of 1−100 pN by moving a permanent magnet up and down at 1 Hz; treatment was 1 Hz daily, for 21 days; and these coated particles were found to enhance proteoglycan matrix, collagen synthesis, and extracellular matrix production
stereocilia of hair cell[158]	force control	electromagnet probe	50 nm cubic magnetic particles were coated with PEG and silica then conjugated to concanavalin A	electromagnet probe was used to apply 0.1 pN of force per magnetic particles in a magnetic-field gradient of 1000 T/m on stereocilia, resulting in the influx of ions into the hair cell
transmembrane receptor of PC-3 cells[159]	force control	permanent magnet	60 nm superparamagnetic particles were cultured with PC-3 prostate cancer cells	cells were exposed to a field of 1.21 T with gradient of 10^4 T/m; endocytosis rate increased by an externally applied magnetic field
intracellular vesicles in rat embryonic cortical neurons cells[160]	force control	permanent magnets	100 nm chitosan-coated magnetic particles	vesicles experienced 6−126 pN under a maximum 150 mT magnetic field
vascular endothelial cadherin (VE-cadherin) and notch receptor[88]	force and position control	three-axis magnetic tweezer was creating by placing a NdFeB permanent magnet on a steel probe tip	50 nm magnetoplasmonic magnetic particles (Zn-doped ferrite core and plasmonc Au shell) were coated with ligand to attach on VE-cadherin and notch receptor	magnetic particles generate a force of 1−9 pN; magnetic force stabilized F-actin to form filamentous networks along with recruitment of vinculin
cortex of HeLa cells[161]	position control	micromagnetic elements were magnetized by a NdFeB permanent magnet	dextran magnetic particles were used	micromagnetic elements permalloy with 1.13 T saturation were patterned on an array
Rac-GTPase signaling in cytoplasm of 3T3 cells and COS7 cells[100]	position control	magnetic tweezer was created by placing a NdFeB permanent magnet on a paramagnetic tip	480 nm superparamagnetic magnetic particles were functionalized with Cdc42(Q61L) or TIAM	magnetic tweezers generate force on magnetic particles up to 70 pN
chromatin stretching through integrin in Chinese hamster ovary cells[92]	torque control	3D magnetic twisting cytometry (3D-MTC)	4 μm magnetic particles were coated with RGD or PLL	coated particles were lifted in 0.1 ms, 2500 G field and twisted at 0.1, 0.3, and 1 Hz in 0−25 G field
rat insulinoma tumor cells and human pancreatic β cells[99]	torque control	dynamic magnetic field generator	100 nm superparamagnetic particles were coated with LAMP1 antibody targeting lysosomal protein	*in vitro*, internalized particles were exposed to 30 mT magnetic field at 10−20 Hz, for 20 min; apoptosis was observed after the treatment
U87 glioblastoma cells[95]	torque control	permanent magnets	62 nm cubic magnetic particles were coated with epidermal growth factor peptide	magnetic particles formed elongated aggregates in lysosomes. *In vitro*, two permanent magnets were installed in a rotating cylinder to apply rotational magnetic field of 40 mT at 15 Hz to tumor cells, and cell membrane rupture, lysosomal membrane rupture, and apoptosis were observed
U87 glioblastoma cells[96]	torque control	NdFeB permanent magnet	2 μm disk-shaped magnetic particles (5 nm Au/60 nm permalloy/5 nm Au) were internalized by glioma cells *in vitro* and *in vivo*	Using a NdFeB permanent magnet mounted on a motor, *in vitro*, the cells were treated with 1 T rotating magnetic field at 20 Hz for 30 min. As for *in vivo* study, the cells were treated 1 h for 7 days, and apoptosis and decrease of brain tumor size were observed
HeLa cells[97]	force and oscillation control	a pair of electromagnetic coils	150−350 nm permalloy magnetic particles were cultured with HeLa cells	each group of cells was exposed to 5−25 mT uniform magnetic field or 12.4 T/m magnetic-field gradient or 0.17−3.33 Hz alternating magnetic field, and apoptosis was observed due to the activation of mechanosensitive ion channels in uniform or magnetic-field gradient
HCT116 colon cancer cells[98]	oscillation control	nanowires, VSM model MicroMag 3900	35 nm diameter nickel nanowires	35 nm diameter nickel nanowires were combined with a 0.5 mT and 1 Hz or 1 kHz alternating magnetic field as cancer cells treatment, and cell membrane leakage and apoptosis were observed
FcεRI receptor of RBL-2H3 mast cells[86]	aggregation control	electromagnetic microneedle	30 nm dinitrophenyl (DNP)-coated magnetic particles adhered to FcεRI receptors through bound anti-DNP IgE antibodies	Magnetic particles were clustered by applying magnetic field, causing the oligomerization and calcium signaling

https://dx.doi.org/10.1021/acsnano.0c00959
ACS Nano 2020, 14, 3805−3821

Table 3. continued

stimulation target	technique	system description	magnetic material	parameters
death receptor 4 of DLD-1 colon cancer cells and zebrafish[52]	aggregation control	magnetic tweezers fabricated by two NdFeB magnets	15 nm magnetic particles were coated with antibody for death receptor 4	A magnetic field of 0.2 T was applied for 2 h, and apoptosis signaling was observed in *in vitro* and *in vivo* system
TRPV1 of HEK293 cells; hippocampal neuron; *C. elegans*[87]	heating control	25-turn solenoid coil	6 nm diameter $MnFe_2O_4$ conjugated with streptavidin form AP-CFP-TM binding with TRPV1	A 40 MHz, 8.4G alternating magnetic field was applied; thermal activation of TRPV1 increases intracellular calcium of HEK293, induces action potential in neurons, and triggers response in worms
TPRV1 of HEK293T cells; mouse mesenchymal stem cells[102]	heating control; force control	2-turn solenoid coil (radius 2.5 cm)	ferritin genetically encoded to be directly tethered to TRPV1	ferritin was genetically encoded to be directly tethered to TRPV1 and exposed to an alternating field of 29−32 mT and 465 kHz; field treatment significantly increased plasma insulin in mice, and static magnetic field was shown to be able to gate a ferritin-tethered TPRV1 channel in *in vitro* and *in vivo* through magnetic force instead of heating control

PDL-1,[118] remain to be tested to understand their mechanical sensitivity and effect for therapeutics. The rotation of magnetic particles[95] and magnetic carbon nanotubes[96] actuated by a rotating magnetic field was reported to mechanically tear intracellular structures and cause cell death. Using intracellular magnetic stimulation to mechanically disrupt cellular structures for therapeutics can potentially circumvent the resistance issues[97] in present cancer treatments.

Surface coating of magnetic particles (Figure 4b) would enable magnetic treatment to more precisely target cancer cells and minimize undesired effects to healthy cells. Recent work has also shown the use of engineered ferritin, a protein that contains iron, synthesized with target antibodies and fluorescent labels, to replace the iron nanoparticles and its surface fictionalization for target intracellular manipulations.[119] For hyperthermia treatment, the use of an alternating magnetic field and magnetic particles, compared with the use of gold nanoparticles and infrared light excitations,[120,121] has the distinct advantage of position control due to the capability of actively locomoting magnetic particles *in vivo*. However, how magnetic particles can be more effectively delivered deep in a tumor and how they are internalized/transported to cancer cells, such as through blood vessels, remain to be better understood and mastered.[122]

Beyond Measurement and Stimulation: Targeted Delivery with Magnetic Micro/nanorobots. Magnetically controlled micro/nanorobots have been applied to targeted drug and cell delivery[123] and assisted fertilization.[124] Inspired by bacterial flagella, magnetic helical swimmers were used to provide propulsion toward a target location under a rotating magnetic field.[125] Biological entities such as sperm,[126−128] microalga,[129] and bacteria,[112,130,131] which are equipped with molecular motility machineries for effective navigation in a complex environment, have also been adopted to provide propulsion for targeted delivery, under steering control from an external magnetic field. For the fabrication of micro-objects with porous structures for targeted delivery, natural materials were used as templates, ranging from pollen (*e.g.*, pine pollen),[132] bacteria (*e.g.*, *Streptomyces platensis*),[114] to fungi (*e.g.*, *Ganoderma lucidum*).[133] For cell delivery, magnetic microrobots were fabricated using 3D laser lithography to form scaffolds for cell attachment.[134,135] These microrobots were shown to be moved and positioned *in vivo* (*e.g.*, in the cartilage of a rabbit knee) *via* magnetic control.[136,137] For lowering toxicity, the synthesis of biodegradable polymers for the construction of micro/nanorobots has been a focus of recent research for targeted drug and cell delivery.[138,139]

Biocompatibility and Biodegradability of Magnetic Particles. Despite the wide applications of magnetic nanoparticles for cellular measurement, stimulation, and therapies, their long-term intracellular fate remains under explored.[140] It was shown that the cell membrane accounted for the internalization of nanoparticles into a cell,[141] and the internalization process was affected by the size, shape, surface charge, coating, and hydrophobicity of the particles.[142,143] After internalized, magnetic nanoparticles are degraded in the endosomes of cells by a number of hydrolytic enzymes such as the lysosomal Cathepsin L, as shown both *in vitro* and *in vivo*.[144] The release of reactive iron species during degradation can be a source of cytotoxicity.[140,145] To address the cytotoxicity issue, surface coating of nanoparticles with more biocompatible materials (*e.g.*, carbon[146] and gold[147]) were used; biopolymers were developed to encapsulate magnetic

https://dx.doi.org/10.1021/acsnano.0c00959
ACS Nano 2020, 14, 3805−3821

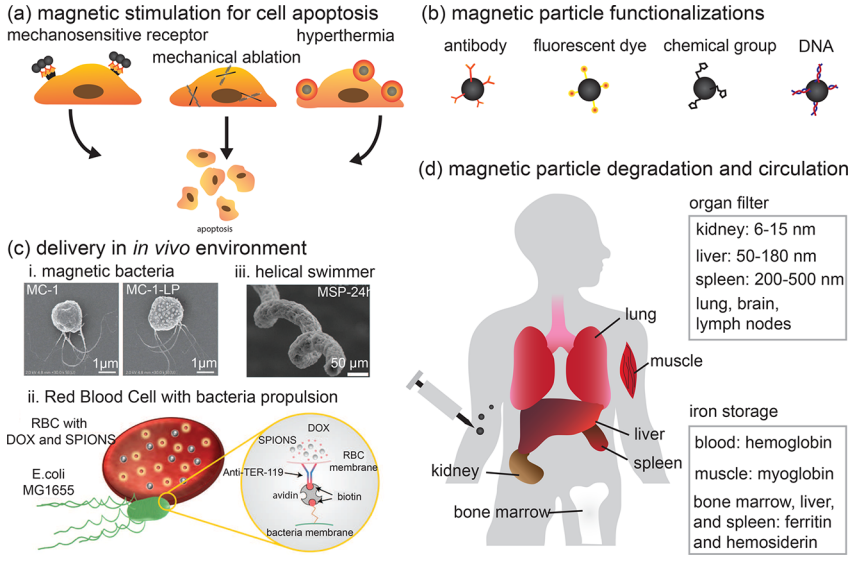

Figure 4. (a) Mechanical stimulation of cancer cells for treatment: stimulation of mechanosensitive receptors on cell surface, mechanical ablation using rotating magnetic tubes/rods, and hyperthermia treatment using heat generated on magnetic particles. (b) Biochemical functionalization of magnetic particles. (c) (i) Target delivery using magneto-bacteria. Adapted with permission from ref 112. Copyright 2016 Springer Nature. (ii) Target delivery using magnetic particles. Adapted with permission from ref 113. Copyright 2018 AAAS. (iii) Target delivery using helical-shaped *Spirulina*. Adapted with permission from ref 114. Copyright 2017 AAAS. (d) Iron circulation and storage inside the human body after introducing iron magnetic particles through intravenous injection. Reproduced with permission from ref 115. Copyright 2015 Royal Society of Chemistry.

nanoparticles;[139] and the protein, ferritin, was used as a replacement of iron particles.[119]

For *in vivo* applications, the degradation of magnetic particles and related toxic effects requires further research.[23,25,148,149] In clinical applications of magnetic micromanipulation, sufficient propelling forces are needed for navigating magnetic particles or devices inside the body to reach the target location, for example, inside the bloodstream or penetrate deep into tumors for drug delivery. Biohybrid magnetic microrobots have been developed which utilize inherent propulsion from swarms of magneto-bacteria to carry cargos (*e.g.*, drugs), while the magnetic field was used to guide their motion direction[112,128−130] (Figure 4c). In the pursuit of magnetic materials with better biocompatibility, biodegradable materials have become a focus in recent studies of magnetically actuated microrobots.[113,114,150] For instance, biohybrid magnetic helical swimmers were formed through coating magnetic nanoparticles onto the surface of *S. platensis*. When a rotatory magnetic field was applied, the *S. platensis* coated with magnetic nanoparticles generated propulsion toward the delivery site.[114] Regarding safety, once introduced into the body (*e.g.*, through intravenous injection), magnetic particles would be taken by organs such as kidney, liver, lung, and spleen,[151] and the remaining iron inside the blood would be degraded and stored in bone marrow, hemoglobin in red blood cells, myoglobin in muscle tissues, *etc.*[115] (Figure 4d). The safety requirements for *in vivo* applications require the magnetic particles or devices to be traceable, biocompatible, and retractable or largely biodegradable. The next decade will witness more intense efforts in the magnetic material development, integration of magnetic micromanipulation, and imaging modalities (*e.g.*, CT, MRI, ultrasound, super-resolution fluorescence imaging)[152,153] with advanced imaging modalities for imaging at deep tissue for tracking the micro and nanoscale objects,[154,155] and the magnetic control techniques for precise delivery and surgery tasks.

AUTHOR INFORMATION

Corresponding Author

Yu Sun − *Department of Mechanical and Industrial Engineering, Institute of Biomaterials and Biomedical Engineering, and Department of Electrical and Computer Engineering, University of Toronto, Toronto, Ontario M5S 3G8, Canada;* orcid.org/0000-0001-7895-0741; Email: sun@mie.utoronto.ca

Authors

Xian Wang − *Department of Mechanical and Industrial Engineering and Institute of Biomaterials and Biomedical Engineering, University of Toronto, Toronto, Ontario M5S 3G8, Canada;* orcid.org/0000-0002-1501-2544

Junhui Law − *Department of Mechanical and Industrial Engineering, University of Toronto, Toronto, Ontario M5S 3G8, Canada;* orcid.org/0000-0002-6033-7639

Mengxi Luo − *Department of Mechanical and Industrial Engineering, University of Toronto, Toronto, Ontario M5S 3G8, Canada*

Zheyuan Gong − *Department of Mechanical and Industrial Engineering, University of Toronto, Toronto, Ontario M5S 3G8, Canada;* orcid.org/0000-0002-8739-5222

Jiangfan Yu − *Department of Mechanical and Industrial Engineering, University of Toronto, Toronto, Ontario M5S 3G8, Canada*

Wentian Tang − *Department of Mechanical and Industrial Engineering, University of Toronto, Toronto, Ontario M5S 3G8, Canada;* orcid.org/0000-0003-1454-2022

Zhuoran Zhang − *Department of Mechanical and Industrial Engineering, University of Toronto, Toronto, Ontario M5S 3G8, Canada;* orcid.org/0000-0002-8737-4210

Xueting Mei − *Department of Mechanical and Industrial Engineering and Institute of Biomaterials and Biomedical Engineering, University of Toronto, Toronto, Ontario M5S 3G8, Canada*

https://dx.doi.org/10.1021/acsnano.0c00959
ACS Nano 2020, 14, 3805−3821

Zongjie Huang − *Department of Mechanical and Industrial Engineering, University of Toronto, Toronto, Ontario M5S 3G8, Canada;* orcid.org/0000-0001-9731-8215

Lidan You − *Department of Mechanical and Industrial Engineering and Institute of Biomaterials and Biomedical Engineering, University of Toronto, Toronto, Ontario M5S 3G8, Canada*

Complete contact information is available at: https://pubs.acs.org/10.1021/acsnano.0c00959

Notes

The authors declare no competing financial interest.

ACKNOWLEDGMENTS

This work was supported by the National Sciences and Engineering Research Council of Canada *via* an NSERC Discovery Grant, by the Ontario Research Fund *via* the Research Excellence Program, by the Canada Research Chairs program.

VOCABULARY

Magnetic nanoparticles, a class of nanoparticles typically smaller than 1 μm in diameter and also responsive to magnetic fields, commonly consist of magnetic materials (*i.e.*, iron, nickel, cobalt, and their alloys) and surface coating (gold, carbon, *etc.*) or functionalization (*e.g.*, antibodies, DNA strand); **magnetic torque**, a vector relating the aligning torque on an object from the external magnetic field toward the direction of the field strength; **magnetic dipole**, a magnetic analogue of the electric dipole, describes either a closed loop of current or a pair of poles as the size of the source is close to zero while keeping the magnetic moment constant; **hyperthermia**, a type of cancer treatment, which utilizes high temperature to cause cancer cell death while minimizing the damage to the healthy cells. It is also called thermotherapy; **cytotoxicity**, a quality of being toxic to cells, usually quantified by cell death rate/ratio calculated from cytotoxicity assays (*e.g.*, trypan blue staining)

REFERENCES

(1) Kumar, S.; Weaver, V. M. Mechanics, Malignancy, and Metastasis: The Force Journey of a Tumor Cell. *Cancer Metastasis Rev.* **2009**, *28*, 113−127.
(2) Martinac, B. Mechanosensitive Ion Channels: Molecules of Mechanotransduction. *J. Cell Sci.* **2004**, *117*, 2449−2460.
(3) Garzon-Coral, C.; Fantana, H. A.; Howard, J. A Force-Generating Machinery Maintains the Spindle at the Cell Center During Mitosis. *Science* **2016**, *352*, 1124−1127.
(4) Settembre, C.; Ballabio, A. Lysosomal Adaptation: How the Lysosome Responds to External Cues. *Cold Spring Harbor Perspect. Biol.* **2014**, *6*, a016907.
(5) McNeil, P. L. Repairing a Torn Cell Surface: Make Way, Lysosomes to the Rescue. *J. Cell Sci.* **2002**, *115*, 873−879.
(6) Schönthal, A. H. Endoplasmic Reticulum Stress: Its Role in Disease and Novel Prospects for Therapy. *Scientifica* **2012**, *2012*, 857516.
(7) Dahl, K. N.; Ribeiro, A. J.; Lammerding, J. Nuclear Shape, Mechanics, and Mechanotransduction. *Circ. Res.* **2008**, *102*, 1307−1318.
(8) Denais, C. M.; Gilbert, R. M.; Isermann, P.; McGregor, A. L.; Te Lindert, M.; Weigelin, B.; Davidson, P. M.; Friedl, P.; Wolf, K.; Lammerding, J. Nuclear Envelope Rupture and Repair During Cancer Cell Migration. *Science* **2016**, *352*, 353−358.
(9) Vining, K. H.; Mooney, D. J. Mechanical Forces Direct Stem Cell Behaviour in Development and Regeneration. *Nat. Rev. Mol. Cell Biol.* **2017**, *18*, 728.
(10) Liu, J.; Wen, J.; Zhang, Z.; Liu, H.; Sun, Y. Voyage Inside the Cell: Microsystems and Nanoengineering for Intracellular Measurement and Manipulation. *Microsyst. Nanoeng.* **2015**, *1*, 15020.
(11) Bao, G.; Kamm, R. D.; Thomas, W.; Hwang, W.; Fletcher, D. A.; Grodzinsky, A. J.; Zhu, C.; Mofrad, M. R. Molecular Biomechanics: The Molecular Basis of How Forces Regulate Cellular Function. *Cell. Mol. Bioeng.* **2010**, *3*, 91−105.
(12) Davidson, P. M.; Lammerding, J. Broken Nuclei−Lamins, Nuclear Mechanics, and Disease. *Trends Cell Biol.* **2014**, *24*, 247−256.
(13) Schuerle, S.; Vizcarra, I. A.; Moeller, J.; Sakar, M. S.; Özkale, B.; Lindo, A. M.; Mushtaq, F.; Schoen, I.; Pané, S.; Vogel, V.; Nelson, B. J. Robotically Controlled Microprey to Resolve Initial Attack Modes Preceding Phagocytosis. *Sci. Rob.* **2017**, *2*, No. eaah6094.
(14) Katrukha, E. A.; Mikhaylova, M.; van Brakel, H. X.; en Henegouwen, P. M. v. B.; Akhmanova, A.; Hoogenraad, C. C.; Kapitein, L. C. Probing Cytoskeletal Modulation of Passive and Active Intracellular Dynamics Using Nanobody-Functionalized Quantum Dots. *Nat. Commun.* **2017**, *8*, 14772.
(15) Wang, X.; Liu, H.; Zhu, M.; Cao, C.; Xu, Z.; Tsatskis, Y.; Lau, K.; Kuok, C.; Filleter, T.; McNeill, H.; Simmons, C. A.; Hopyan, S.; Sun, Y. Mechanical Stability of the Cell Nucleus−Roles Played by the Cytoskeleton in Nuclear Deformation and Strain Recovery. *J. Cell Sci.* **2018**, *131*, jcs209627.
(16) Hosu, B. G.; Jakab, K.; Bánki, P.; Tóth, F. I.; Forgacs, G. Magnetic Tweezers for Intracellular Applications. *Rev. Sci. Instrum.* **2003**, *74*, 4158−4163.
(17) Li, X.; Liu, C.; Chen, S.; Wang, Y.; Cheng, S. H.; Sun, D. *In Vivo* Manipulation of Single Biological Cells with an Optical Tweezers-Based Manipulator and a Disturbance Compensation Controller. *IEEE Trans. Robot.* **2017**, *33*, 1200−1212.
(18) Wang, W.; Li, S.; Mair, L.; Ahmed, S.; Huang, T. J.; Mallouk, T. E. Acoustic Propulsion of Nanorod Motors inside Living Cells. *Angew. Chem., Int. Ed.* **2014**, *53*, 3201−3204.
(19) Urbano, R. L.; Clyne, A. M. An Inverted Dielectrophoretic Device for Analysis of Attached Single Cell Mechanics. *Lab Chip* **2016**, *16*, 561−573.
(20) Liu, J.; Zhang, Z.; Tao, H.; Ge, J.; Liu, H.; Wen, J.; Hopyan, S.; Pu, H.; Xie, S.; Sun, Y. Robotic Fluidic Jet for Automated Cellular and Intracellular Mechanical Characterization. Proceedings of the *IEEE International Conference on Information and Automation (ICIA)*, Ningbo, China, July 31−August 4, 2016; IEEE: Piscataway, NJ, 2016; pp 462−467.
(21) Wang, X.; Luo, M.; Wu, H.; Zhang, Z.; Liu, J.; Xu, Z.; Johnson, W.; Sun, Y. A Three-Dimensional Magnetic Tweezer System for Intraembryonic Navigation and Measurement. *IEEE Trans. Robot.* **2018**, *34*, 240−247.
(22) Wang, X.; Ho, C.; Tsatskis, Y.; Law, J.; Zhang, Z.; Zhu, M.; Dai, C.; Wang, F.; Tan, M.; Hopyan, S.; McNeill, H.; Sun, Y. Intracellular Manipulation and Measurement with Multipole Magnetic Tweezers. *Sci. Rob.* **2019**, *4*, No. eaav6180.
(23) Chen, X.-Z.; Hoop, M.; Mushtaq, F.; Siringil, E.; Hu, C.; Nelson, B. J.; Pané, S. Recent Developments in Magnetically Driven Micro- and Nanorobots. *Appl. Mater. Today* **2017**, *9*, 37−48.
(24) Chen, X.-Z.; Jang, B.; Ahmed, D.; Hu, C.; De Marco, C.; Hoop, M.; Mushtaq, F.; Nelson, B. J.; Pané, S. Small-Scale Machines Driven by External Power Sources. *Adv. Mater.* **2018**, *30*, 1705061.
(25) Zhang, Y.; Yuan, K.; Zhang, L. Micro/Nanomachines: From Functionalization to Sensing and Removal. *Adv. Mater. Technol.* **2019**, *4*, 1800636.
(26) Li, J.; de Ávila, B. E.-F.; Gao, W.; Zhang, L.; Wang, J. Micro/Nanorobots for Biomedicine: Delivery, Surgery, Sensing, and Detoxification. *Sci. Rob.* **2017**, *2*, eaam6431.
(27) Monzel, C.; Vicario, C.; Piehler, J.; Coppey, M.; Dahan, M. Magnetic Control of Cellular Processes Using Biofunctional Nanoparticles. *Chem. Sci.* **2017**, *8*, 7330−7338.

(28) Ryan, P.; Diller, E. Magnetic Actuation for Full Dexterity Microrobotic Control Using Rotating Permanent Magnets. *IEEE Trans. on Robot.* **2017**, *33*, 1398−1409.
(29) Schuerle, S.; Erni, S.; Flink, M.; Kratochvil, B. E.; Nelson, B. J. Three-Dimensional Magnetic Manipulation of Micro- and Nanostructures for Applications in Life Sciences. *IEEE Trans. Magn.* **2013**, *49*, 321−330.
(30) Kummer, M. P.; Abbott, J. J.; Kratochvil, B. E.; Borer, R.; Sengul, A.; Nelson, B. J. OctoMag: An Electromagnetic System for 5-DOF Wireless Micromanipulation. *IEEE Trans. on Robot.* **2010**, *26*, 1006−1017.
(31) Yang, L.; Du, X.; Yu, E.; Jin, D.; Zhang, L. DeltaMag: An Electromagnetic Manipulation System with Parallel Mobile Coils. Proceedings of the *IEEE International Conference on Robotics and Automation (ICRA)*, Montreal, Canada, May 20−24, 2019;IEEE: Piscataway, NJ, 2019; pp 9814−9820.
(32) Vonthron, M.; Lalande, V.; Bringout, G.; Tremblay, C.; Martel, S. A MRI-Based Integrated Platform for the Navigation of Micro-Devices and Microrobots. Proceedings of the *IEEE/RSJ International Conference on Intelligent Robots and Systems (IROS)*, San Francisco, CA, September 25−30, 2011; IEEE: Piscataway, NJ, 2011; pp 1285−1290.
(33) Vartholomeos, P.; Bergeles, C.; Qin, L.; Dupont, P. E. An MRI-Powered and Controlled Actuator Technology for Tetherless Robotic Interventions. *Int. J. Robot. Res.* **2013**, *32*, 1536−1552.
(34) Liu, T.; Jackson, R.; Franson, D.; Poirot, N. L.; Criss, R. K.; Seiberlich, N.; Griswold, M. A.; Çavuşoğlu, M. C. Iterative Jacobian-Based Inverse Kinematics and Open-Loop Control of an MRI-Guided Magnetically Actuated Steerable Catheter System. *IEEE/ASME Trans. Mechatronics* **2017**, *22*, 1765−1776.
(35) Wilson, M. W.; Martin, A. B.; Lillaney, P.; Losey, A. D.; Yee, E. J.; Bernhardt, A.; Malba, V.; Evans, L.; Sincic, R.; Saeed, M.; Arenson, R. L.; Hetts, S. W. Magnetic Catheter Manipulation in the Interventional MR Imaging Environment. *J. Vasc. Interv. Radiol.* **2013**, *24*, 885−891.
(36) Zhang, Z.; Huang, K.; Menq, C.-H. Design, Implementation, and Force Modeling of Quadrupole Magnetic Tweezers. *IEEE/ASME Trans. Mechatronics* **2010**, *15*, 704−713.
(37) Spaldin, N. A. *Paramagnetism. Magnetic Materials: Fundamentals and Applications*; Cambridge University Press: Cambridge, England, 2010; pp 48−64.
(38) Tadic, M.; Kralj, S.; Jagodic, M.; Hanzel, D.; Makovec, D. Magnetic Properties of Novel Superparamagnetic IRON Oxide Nanoclusters and Their Peculiarity under Annealing Treatment. *Appl. Surf. Sci.* **2014**, *322*, 255−264.
(39) Alenghat, F. J.; Fabry, B.; Tsai, K. Y.; Goldmann, W. H.; Ingber, D. E. Analysis of Cell Mechanics in Single Vinculin-Deficient Cells Using a Magnetic Tweezer. *Biochem. Biophys. Res. Commun.* **2000**, *277*, 93−99.
(40) Tajik, A.; Zhang, Y.; Wei, F.; Sun, J.; Jia, Q.; Zhou, W.; Singh, R.; Khanna, N.; Belmont, A. S.; Wang, N. Transcription Upregulation *via* Force-Induced Direct Stretching of Chromatin. *Nat. Mater.* **2016**, *15*, 1287.
(41) Predescu, A. M.; Matei, E.; Berbecaru, A. C.; Pantilimon, C.; Drăgan, C.; Vidu, R.; Predescu, C.; Kuncser, V. Synthesis and Characterization of Dextran-Coated IRON Oxide Nanoparticles. *R. Soc. Open Sci.* **2018**, *5*, 171525.
(42) Cotin, G.; Piant, S.; Mertz, D.; Felder-Flesch, D.; Begin-Colin, S. *Iron Oxide Nanoparticles for Biomedical Applications: Synthesis, Functionalization, and Application. Iron Oxide Nanoparticles for Biomedical Applications*; Elsevier: Amsterdam, Netherlands, 2018; pp 43−88.
(43) Suk, J. S.; Xu, Q.; Kim, N.; Hanes, J.; Ensign, L. M. PEGylation as a Strategy for Improving Nanoparticle-Based Drug and Gene Delivery. *Adv. Drug Delivery Rev.* **2016**, *99*, 28−51.
(44) Xu, C.; Xu, K.; Gu, H.; Zhong, X.; Guo, Z.; Zheng, R.; Zhang, X.; Xu, B. Nitrilotriacetic Acid-Modified Magnetic Nanoparticles as a General Agent to Bind Histidine-Tagged Proteins. *J. Am. Chem. Soc.* **2004**, *126*, 3392−3393.
(45) Singh, H.; Laibinis, P. E.; Hatton, T. A. Rigid, Superparamagnetic Chains of Permanently Linked Beads Coated With Magnetic Nanoparticles. Synthesis and Rotational Dynamics Under Applied Magnetic Fields. *Langmuir* **2005**, *21*, 11500−11509.
(46) Jia, D.; Hamilton, J.; Zaman, L. M.; Goonewardene, A. The Time, Size, Viscosity, and Temperature Dependence of the Brownian Motion of Polystyrene Microspheres. *Am. J. Phys.* **2007**, *75*, 111−115.
(47) Diller, E.; Sitti, M. Micro-Scale Mobile Robotics. *Found. Trends Robot.* **2011**, *2*, 143−259.
(48) Bidan, C. M.; Fratzl, M.; Coullomb, A.; Moreau, P.; Lombard, A. H.; Wang, I.; Balland, M.; Boudou, T.; Dempsey, N. M.; Devillers, T.; Dupont, A. Magneto-Active Substrates for Local Mechanical Stimulation of Living Cells. *Sci. Rep.* **2018**, *8*, 1464.
(49) Zahn, C.; Keller, S.; Toro-Nahuelpan, M.; Dorscht, P.; Gross, W.; Laumann, M.; Gekle, S.; Zimmermann, W.; Schüler, D.; Kress, H. Measurement of the Magnetic Moment of Single *Magnetospirillum Gryphiswaldense* Cells by Magnetic Tweezers. *Sci. Rep.* **2017**, *7*, 3558.
(50) Kotani, N.; Gu, J.; Isaji, T.; Udaka, K.; Taniguchi, N.; Honke, K. Biochemical Visualization of Cell Surface Molecular Clustering in Living Cells. *Proc. Natl. Acad. Sci. U. S. A.* **2008**, *105*, 7405−7409.
(51) Yung, K. W.; Landecker, P. B.; Villani, D. D. An Analytic Solution for the Force between Two Magnetic Dipoles. *Magn. Electr. Sep.* **1998**, *9*, 39−52.
(52) Cho, M. H.; Lee, E. J.; Son, M.; Lee, J.-H.; Yoo, D.; Kim, J.-w.; Park, S. W.; Shin, J.-S.; Cheon, J. A Magnetic Switch for the Control of Cell Death Signalling in *In Vitro* and *In Vivo* Systems. *Nat. Mater.* **2012**, *11*, 1038.
(53) Chen, R.; Romero, G.; Christiansen, M. G.; Mohr, A.; Anikeeva, P. Wireless Magnetothermal Deep Brain Stimulation. *Science* **2015**, *347*, 1477−1480.
(54) Chen, R.; Christiansen, M. G.; Anikeeva, P. Maximizing Hysteretic Losses in Magnetic Ferrite Nanoparticles *via* Model-Driven Synthesis and Materials Optimization. *ACS Nano* **2013**, *7*, 8990−9000.
(55) Tong, S.; Quinto, C. A.; Zhang, L.; Mohindra, P.; Bao, G. Size-Dependent Heating of Magnetic IRON Oxide Nanoparticles. *ACS Nano* **2017**, *11*, 6808−6816.
(56) Pearce, J.; Giustini, A.; Stigliano, R.; Jack Hoopes, P. Magnetic Heating of Nanoparticles: The Importance of Particle Clustering to Achieve Therapeutic Temperatures. *J. Nanotechnol. Eng. Med.* **2013**, *4*, 011005.
(57) Giustini, A. J.; Petryk, A. A.; Cassim, S. M.; Tate, J. A.; Baker, I.; Hoopes, P. J. Magnetic Nanoparticle Hyperthermia in Cancer Treatment. *Nano LIFE* **2010**, *1*, 17−32.
(58) Jose, J.; Kumar, R.; Harilal, S.; Mathew, G. E.; Prabhu, A.; Uddin, M. S.; Aleya, L.; Kim, H.; Mathew, B. Magnetic Nanoparticles for Hyperthermia in Cancer Treatment: An Emerging Tool. *Environ. Sci. Pollut. Res.* **2019**, *1*. DOI: 10.1007/s11356-019-07231-2
(59) Chang, D.; Lim, M.; Goos, J. A.; Qiao, R.; Ng, Y. Y.; Mansfeld, F. M.; Jackson, M.; Davis, T. P.; Kavallaris, M. Biologically Targeted Magnetic Hyperthermia: Potential and Limitations. *Front. Pharmacol.* **2018**, *9*, 831.
(60) Crick, F.; Hughes, A. The Physical Properties of Cytoplasm. *Exp. Cell Res.* **1950**, *1*, 37−80.
(61) Strick, T. R.; Allemand, J.-F.; Bensimon, D.; Bensimon, A.; Croquette, V. The Elasticity of a Single Supercoiled DNA Molecule. *Science* **1996**, *271*, 1835−1837.
(62) Fisher, J. K.; Cribb, J.; Desai, K. V.; Vicci, L.; Wilde, B.; Keller, K.; Taylor, R. M.; Haase, J.; Bloom, K.; O'Brien, E. T.; Superfine, R. Thin-Foil Magnetic Force System for High-Numerical-Aperture Microscopy. *Rev. Sci. Instrum.* **2006**, *77*, 023702.
(63) De Vries, A. H.; Krenn, B. E.; van Driel, R.; Kanger, J. S. Micro Magnetic Tweezers for Nanomanipulation inside Live Cells. *Biophys. J.* **2005**, *88*, 2137−2144.
(64) Son, D.; Dogan, M. D.; Sitti, M. Magnetically Actuated Soft Capsule Endoscope for Fine-Needle Aspiration Biopsy. Proceedings of the *IEEE International Conference on Robotics and Automation (ICRA)*, Singapore, May 2−June 3, 2017; IEEE: Piscataway, NJ, 2017; pp 1132−1139.

(65) Zhang, Y.; Wei, F.; Poh, Y.-C.; Jia, Q.; Chen, J.; Chen, J.; Luo, J.; Yao, W.; Zhou, W.; Huang, W.; Yang, F.; Zhang, Y.; Wang, N. Interfacing 3D Magnetic Twisting Cytometry with Confocal Fluorescence Microscopy to Image Force Responses in Living Cells. *Nat. Protoc.* **2017**, *12*, 1437.
(66) Bausch, A. R.; Möller, W.; Sackmann, E. Measurement of Local Viscoelasticity and Forces in Living Cells by Magnetic Tweezers. *Biophys. J.* **1999**, *76*, 573−579.
(67) Guilluy, C.; Osborne, L. D.; Van Landeghem, L.; Sharek, L.; Superfine, R.; Garcia-Mata, R.; Burridge, K. Isolated Nuclei Adapt to Force and Reveal a Mechanotransduction Pathway in the Nucleus. *Nat. Cell Biol.* **2014**, *16*, 376.
(68) Wu, P.-H.; Aroush, D. R.-B.; Asnacios, A.; Chen, W.-C.; Dokukin, M. E.; Doss, B. L.; Durand-Smet, P.; Ekpenyong, A.; Guck, J.; Guz, N. V.; et al. A Comparison of Methods to Assess Cell Mechanical Properties. *Nat. Methods* **2018**, *15*, 491−498.
(69) Bausch, A. R.; Ziemann, F.; Boulbitch, A. A.; Jacobson, K.; Sackmann, E. Local Measurements of Viscoelastic Parameters of Adherent Cell Surfaces by Magnetic Bead Microrheometry. *Biophys. J.* **1998**, *75*, 2038−2049.
(70) Bonakdar, N.; Gerum, R.; Kuhn, M.; Spörrer, M.; Lippert, A.; Schneider, W.; Aifantis, K. E.; Fabry, B. Mechanical Plasticity of Cells. *Nat. Mater.* **2016**, *15*, 1090−1094.
(71) Osborne, L. D.; Li, G. Z.; How, T.; O'Brien, E. T.; Blobe, G. C.; Superfine, R.; Mythreye, K. TGF-β Regulates LARG and GEF-H1 During EMT to Affect Stiffening Response to Force and Cell Invasion. *Mol. Biol. Cell* **2014**, *25*, 3528−3540.
(72) Martini, F. *The Cellular Level of Organization. Fundamentals of Anatomy and Physiology*, 5th ed., Prentice-Hall Inc: New Jersey, 2001; pp 15−24.
(73) Dijksterhuis, J.; Nijsse, J.; Hoekstra, F.; Golovina, E. High Viscosity and Anisotropy Characterize the Cytoplasm of Fungal Dormant Stress-Resistant Spores. *Eukaryotic Cell* **2007**, *6*, 157−170.
(74) Niwayama, R.; Shinohara, K.; Kimura, A. Hydrodynamic Property of the Cytoplasm Is Sufficient to Mediate Cytoplasmic Streaming in the *Caenorhabiditis Elegans* Embryo. *Proc. Natl. Acad. Sci. U. S. A.* **2011**, *108*, 11900−11905.
(75) Berret, J.-F. Local Viscoelasticity of Living Cells Measured by Rotational Magnetic Spectroscopy. *Nat. Commun.* **2016**, *7*, 10134.
(76) Dahl, K. N.; Scaffidi, P.; Islam, M. F.; Yodh, A. G.; Wilson, K. L.; Misteli, T. Distinct Structural and Mechanical Properties of the Nuclear Lamina in Hutchinson−Gilford Progeria Syndrome. *Proc. Natl. Acad. Sci. U. S. A.* **2006**, *103*, 10271−10276.
(77) Lanzicher, T.; Martinelli, V.; Puzzi, L.; Del Favero, G.; Codan, B.; Long, C. S.; Mestroni, L.; Taylor, M. R.; Sbaizero, O. The Cardiomyopathy Lamin A/C D192G Mutation Disrupts Whole-Cell Biomechanics in Cardiomyocytes as Measured by Atomic Force Microscopy Loading-Unloading Curve Analysis. *Sci. Rep.* **2015**, *5*, 13388.
(78) Liu, H.; Wen, J.; Xiao, Y.; Liu, J.; Hopyan, S.; Radisic, M.; Simmons, C. A.; Sun, Y. *In Situ* Mechanical Characterization of the Cell Nucleus by Atomic Force Microscopy. *ACS Nano* **2014**, *8*, 3821−3828.
(79) Lammerding, J.; Dahl, K. N.; Discher, D. E.; Kamm, R. D. Nuclear Mechanics and Methods. *Methods Cell Biol.* **2007**, *83*, 269−294.
(80) Kanger, J. S.; Subramaniam, V.; van Driel, R. Intracellular Manipulation of Chromatin Using Magnetic Nanoparticles. *Chromosome Res.* **2008**, *16*, 511.
(81) Van Oene, M. M.; Dickinson, L. E.; Cross, B.; Pedaci, F.; Lipfert, J.; Dekker, N. H. Applying Torque to the *Escherichia Coli* Flagellar Motor Using Magnetic Tweezers. *Sci. Rep.* **2017**, *7*, 43285.
(82) Fallesen, T. L.; Macosko, J. C.; Holzwarth, G. Force−Velocity Relationship for Multiple Kinesin Motors Pulling a Magnetic Bead. *Eur. Biophys. J.* **2011**, *40*, 1071−1079.
(83) Tanimoto, H.; Sallé, J.; Dodin, L.; Minc, N. Physical Forces Determining the Persistency and Centring Precision of Microtubule Asters. *Nat. Phys.* **2018**, *14*, 848.
(84) Revyakin, A.; Ebright, R. H.; Strick, T. R. Promoter Unwinding and Promoter Clearance by RNA Polymerase: Detection by Single-Molecule DNA Nanomanipulation. *Proc. Natl. Acad. Sci. U. S. A.* **2004**, *101*, 4776−4780.
(85) Wheeler, M. A.; Smith, C. J.; Ottolini, M.; Barker, B. S.; Purohit, A. M.; Grippo, R. M.; Gaykema, R. P.; Spano, A. J.; Beenhakker, M. P.; Kucenas, S.; Patel, M. K.; Deppmann, C. D.; Güler, A. D. Genetically Targeted Magnetic Control of the Nervous System. *Nat. Neurosci.* **2016**, *19*, 756.
(86) Mannix, R. J.; Kumar, S.; Cassiola, F.; Montoya-Zavala, M.; Feinstein, E.; Prentiss, M.; Ingber, D. E. Nanomagnetic Actuation of Receptor-Mediated Signal Transduction. *Nat. Nanotechnol.* **2008**, *3*, 36.
(87) Huang, H.; Delikanli, S.; Zeng, H.; Ferkey, D. M.; Pralle, A. Remote Control of Ion Channels and Neurons through Magnetic-Field Heating of Nanoparticles. *Nat. Nanotechnol.* **2010**, *5*, 602.
(88) Seo, D.; Southard, K. M.; Kim, J.-W.; Lee, H. J.; Farlow, J.; Lee, J.-U.; Litt, D. B.; Haas, T.; Alivisatos, A. P.; Cheon, J.; Gartner, Z. J.; Jun, Y.-W. A Mechanogenetic Toolkit for Interrogating Cell Signaling in Space and Time. *Cell* **2016**, *165*, 1507−1518.
(89) Kilinc, D.; Lesniak, A.; Rashdan, S. A.; Gandhi, D.; Blasiak, A.; Fannin, P. C.; von Kriegsheim, A.; Kolch, W.; Lee, G. U. Mechanochemical Stimulation of MCF7 Cells with Rod-Shaped Fe−Au Janus Particles Induces Cell Death through Paradoxical Hyperactivation of ERK. *Adv. Healthcare Mater.* **2015**, *4*, 395−404.
(90) Rotherham, M.; El Haj, A. J. Remote Activation of the Wnt/β-Catenin Signalling Pathway Using Functionalised Magnetic Particles. *PLoS One* **2015**, *10*, No. e0121761.
(91) Kanczler, J. M.; Sura, H. S.; Magnay, J.; Green, D.; Oreffo, R. O.; Dobson, J. P.; El Haj, A. J. Controlled Differentiation of Human Bone Marrow Stromal Cells Using Magnetic Nanoparticle Technology. *Tissue Eng., Part A* **2010**, *16*, 3241−3250.
(92) Hoffmann, C.; Mazari, E.; Lallet, S.; Le Borgne, R.; Marchi, V.; Gosse, C.; Gueroui, Z. Spatiotemporal Control of Microtubule Nucleation and Assembly Using Magnetic Nanoparticles. *Nat. Nanotechnol.* **2013**, *8*, 199.
(93) Wang, N.; Butler, J. P.; Ingber, D. E. Mechanotransduction Across the Cell Surface and Through the Cytoskeleton. *Science* **1993**, *260*, 1124−1127.
(94) Jordan, A.; Scholz, R.; Wust, P.; Fähling, H.; Krause, J.; Wlodarczyk, W.; Sander, B.; Vogl, T.; Felix, R. Effects of Magnetic Fluid Hyperthermia (MFH) on C3H Mammary Carcinoma *In Vivo*. *Int. J. Hyperthermia* **1997**, *13*, 587−605.
(95) Shen, Y.; Wu, C.; Uyeda, T. Q.; Plaza, G. R.; Liu, B.; Han, Y.; Lesniak, M. S.; Cheng, Y. Elongated Nanoparticle Aggregates in Cancer Cells for Mechanical Destruction with Low Frequency Rotating Magnetic Field. *Theranostics* **2017**, *7*, 1735.
(96) Cheng, Y.; Muroski, M. E.; Petit, D. C.; Mansell, R.; Vemulkar, T.; Morshed, R. A.; Han, Y.; Balyasnikova, I. V.; Horbinski, C. M.; Huang, X.; Zhang, L.; Cowburn, R. P.; Lesniak, M. S. Rotating Magnetic Field Induced Oscillation of Magnetic Particles for *In Vivo* Mechanical Destruction of Malignant Glioma. *J. Controlled Release* **2016**, *223*, 75−84.
(97) Wong, D. W.; Gan, W. L.; Teo, Y. K.; Lew, W. S. Interplay of Cell Death Signaling Pathways Mediated by Alternating Magnetic Field Gradient. *Cell Death Discovery* **2018**, *4*, 49.
(98) Contreras, M. F.; Sougrat, R.; Zaher, A.; Ravasi, T.; Kosel, J. Non-Chemotoxic Induction of Cancer Cell Death Using Magnetic Nanowires. *Int. J. Nanomed.* **2015**, *10*, 2141.
(99) Zhang, E.; Kircher, M. F.; Koch, M.; Eliasson, L.; Goldberg, S. N.; Renström, E. Dynamic Magnetic Fields Remote-Control Apoptosis *via* Nanoparticle Rotation. *ACS Nano* **2014**, *8*, 3192−3201.
(100) Etoc, F.; Lisse, D.; Bellaiche, Y.; Piehler, J.; Coppey, M.; Dahan, M. Subcellular Control of Rac-GTPase Signalling by Magnetogenetic Manipulation inside Living Cells. *Nat. Nanotechnol.* **2013**, *8*, 193.
(101) Stanley, S. A.; Gagner, J. E.; Damanpour, S.; Yoshida, M.; Dordick, J. S.; Friedman, J. M. Radio-Wave Heating of IRON Oxide

https://dx.doi.org/10.1021/acsnano.0c00959
ACS Nano 2020, 14, 3805−3821

Nanoparticles Can Regulate Plasma Glucose in Mice. *Science* **2012**, *336*, 604−608.
(102) Stanley, S. A.; Sauer, J.; Kane, R. S.; Dordick, J. S.; Friedman, J. M. Remote Regulation of Glucose Homeostasis in Mice Using Genetically Encoded Nanoparticles. *Nat. Med.* **2015**, *21*, 92.
(103) Stanley, S. A.; Kelly, L.; Latcha, K. N.; Schmidt, S. F.; Yu, X.; Nectow, A. R.; Sauer, J.; Dyke, J. P.; Dordick, J. S.; Friedman, J. M. Bidirectional Electromagnetic Control of the Hypothalamus Regulates Feeding and Metabolism. *Nature* **2016**, *531*, 647.
(104) Bettaieb, A.; Wrzal, P. K.; Averill-Bates, D. A. *Hyperthermia: Cancer Treatment and Beyond. Cancer Treatment - Conventional and Innovative Approaches*; IntechOpen: London, United Kingdom, 2013; pp 257−283.
(105) Ahmed, K.; Tabuchi, Y.; Kondo, T. Hyperthermia: An Effective Strategy to Induce Apoptosis in Cancer Cells. *Apoptosis* **2015**, *20*, 1411−1419.
(106) Dutz, S.; Hergt, R. Magnetic Nanoparticle Heating and Heat Transfer on a Microscale: Basic Principles, Realities and Physical Limitations of Hyperthermia for Tumour Therapy. *Int. J. Hyperthermia* **2013**, *29*, 790−800.
(107) Hayashi, K.; Nakamura, M.; Miki, H.; Ozaki, S.; Abe, M.; Matsumoto, T.; Sakamoto, W.; Yogo, T.; Ishimura, K. Magnetically Responsive Smart Nanoparticles for Cancer Treatment with a Combination of Magnetic Hyperthermia and Remote-Control Drug Release. *Theranostics* **2014**, *4*, 834.
(108) Asin, L.; Ibarra, M.; Tres, A.; Goya, G. Controlled Cell Death by Magnetic Hyperthermia: Effects of Exposure Time, Field Amplitude, and Nanoparticle Concentration. *Pharm. Res.* **2012**, *29*, 1319−1327.
(109) Prasad, N.; Rathinasamy, K.; Panda, D.; Bahadur, D. Mechanism of Cell Death Induced by Magnetic Hyperthermia with Nanoparticles of γ-Mn x Fe 2−x O 3 Synthesized by a Single Step Process. *J. Mater. Chem.* **2007**, *17*, 5042−5051.
(110) Gordon, R.; Hines, J.; Gordon, D. Intracellular Hyperthermia a Biophysical Approach to Cancer Treatment *via* Intracellular Temperature and Biophysical Alterations. *Med. Hypotheses* **1979**, *5*, 83−102.
(111) Vasan, N.; Baselga, J.; Hyman, D. M. A View on Drug Resistance in Cancer. *Nature* **2019**, *575*, 299−309.
(112) Felfoul, O.; Mohammadi, M.; Taherkhani, S.; De Lanauze, D.; Xu, Y. Z.; Loghin, D.; Essa, S.; Jancik, S.; Houle, D.; Lafleur, M.; Gaboury, L.; Tabrizian, M.; Kaou, N.; Atkin, M.; Vuong, T.; Batist, G.; Beauchemin, N.; Radzioch, D.; Martel, S. Magneto-Aerotactic Bacteria Deliver Drug-Containing Nanoliposomes to Tumour Hypoxic Regions. *Nat. Nanotechnol.* **2016**, *11*, 941.
(113) Alapan, Y.; Yasa, O.; Schauer, O.; Giltinan, J.; Tabak, A. F.; Sourjik, V.; Sitti, M. Soft Erythrocyte-Based Bacterial Microswimmers for Cargo Delivery. *Sci. Rob.* **2018**, *3*, No. eaar4423.
(114) Yan, X.; Zhou, Q.; Vincent, M.; Deng, Y.; Yu, J.; Xu, J.; Xu, T.; Tang, T.; Bian, L.; Wang, Y.-X. J.; Kostarelos, K.; Zhang, L. Multifunctional Biohybrid Magnetite Microrobots for Imaging-Guided Therapy. *Sci. Rob.* **2017**, *2*, No. eaaq1155.
(115) Arami, H.; Khandhar, A.; Liggitt, D.; Krishnan, K. M. *In Vivo* Delivery, Pharmacokinetics, Biodistribution and Toxicity of IRON Oxide Nanoparticles. *Chem. Soc. Rev.* **2015**, *44*, 8576−8607.
(116) Yoshimaru, T.; Suzuki, Y.; Inoue, T.; Nishida, S.; Ra, C. Extracellular Superoxide Released from Mitochondria Mediates Mast Cell Death by Advanced Glycation End Products. *Biochim. Biophys. Acta, Mol. Cell Res.* **2008**, *1783*, 2332−2343.
(117) Pedoeem, A.; Azoulay-Alfaguter, I.; Strazza, M.; Silverman, G. J.; Mor, A. Programmed Death-1 Pathway in Cancer and Autoimmunity. *Clin. Immunol.* **2014**, *153*, 145−152.
(118) Velcheti, V.; Schalper, K. A.; Carvajal, D. E.; Anagnostou, V. K.; Syrigos, K. N.; Sznol, M.; Herbst, R. S.; Gettinger, S. N.; Chen, L.; Rimm, D. L. Programmed Death Ligand-1 Expression in Non-Small Cell Lung Cancer. *Lab. Invest.* **2014**, *94*, 107.
(119) Liße, D.; Monzel, C.; Vicario, C.; Manzi, J.; Maurin, I.; Coppey, M.; Piehler, J.; Dahan, M. Engineered Ferritin for Magnetogenetic Manipulation of Proteins and Organelles inside Living Cells. *Adv. Mater.* **2017**, *29*, 1700189.
(120) Park, H.; Lim, D.-J.; Vines, J. B.; Yoon, J.-H.; Ryu, N.-E. Gold Nanoparticles for Photothermal Cancer Therapy. *Front. Chem.* **2019**, *7*, 167.
(121) Hainfeld, J. F.; Lin, L.; Slatkin, D. N.; Dilmanian, F. A.; Vadas, T. M.; Smilowitz, H. M. Gold Nanoparticle Hyperthermia Reduces Radiotherapy Dose. *Nanomedicine (N. Y., NY, U. S.)* **2014**, *10*, 1609−1617.
(122) Sindhwani, S.; Syed, A. M.; Ngai, J.; Kingston, B. R.; Maiorino, L.; Rothschild, J.; Macmillan, P.; Zhang, Y.; Rajesh, N. U.; Hoang, T.; Wu, J. L. Y.; Wilhelm, S.; Zilman, A.; Gadde, S.; Sulaiman, A.; Ouyang, B.; Lin, Z.; Wang, L.; Egeblad, M.; Chan, W. C. W. The Entry of Nanoparticles into Solid Tumours. *Nat. Mater.* **2020**, DOI: 10.1038/s41563-019-0566-2
(123) Huang, H.-W.; Uslu, F. E.; Katsamba, P.; Lauga, E.; Sakar, M. S.; Nelson, B. J. Adaptive Locomotion of Artificial Microswimmers. *Sci. Adv.* **2019**, *5*, No. eaau1532.
(124) Medina-Sánchez, M.; Schwarz, L.; Meyer, A. K.; Hebenstreit, F.; Schmidt, O. G. Cellular Cargo Delivery: Toward Assisted Fertilization by Sperm-Carrying Micromotors. *Nano Lett.* **2016**, *16*, 555−561.
(125) Peyer, K. E.; Zhang, L.; Nelson, B. J. Bio-Inspired Magnetic Swimming Microrobots for Biomedical Applications. *Nanoscale* **2013**, *5*, 1259−1272.
(126) Magdanz, V.; Sanchez, S.; Schmidt, O. G. Development of a Sperm-Flagella Driven Micro-Bio-Robot. *Adv. Mater.* **2013**, *25*, 6581−6588.
(127) Magdanz, V.; Medina-Sánchez, M.; Schwarz, L.; Xu, H.; Elgeti, J.; Schmidt, O. G. *Spermatozoa* as Functional Components of Robotic Microswimmers. *Adv. Mater.* **2017**, *29*, 1606301.
(128) Xu, H.; Medina-Sánchez, M.; Magdanz, V.; Schwarz, L.; Hebenstreit, F.; Schmidt, O. G. Sperm-Hybrid Micromotor for Targeted Drug Delivery. *ACS Nano* **2018**, *12*, 327−337.
(129) Yasa, O.; Erkoc, P.; Alapan, Y.; Sitti, M. Microalga-Powered Microswimmers toward Active Cargo Delivery. *Adv. Mater.* **2018**, *30*, 1804130.
(130) Stanton, M. M.; Simmchen, J.; Ma, X.; Miguel-López, A.; Sánchez, S. Biohybrid Janus Motors Driven by *Escherichia Coli*. *Adv. Mater. Interfaces* **2016**, *3*, 1500505.
(131) Carlsen, R. W.; Edwards, M. R.; Zhuang, J.; Pacoret, C.; Sitti, M. Magnetic Steering Control of Multi-Cellular Bio-Hybrid Microswimmers. *Lab Chip* **2014**, *14*, 3850−3859.
(132) Sun, M.; Fan, X.; Meng, X.; Song, J.; Chen, W.; Sun, L.; Xie, H. Magnetic Biohybrid Micromotors with High Maneuverability for Efficient Drug Loading and Targeted Drug Delivery. *Nanoscale* **2019**, *11*, 18382−18392.
(133) Zhang, Y.; Zhang, L.; Yang, L.; Vong, C. I.; Chan, K. F.; Wu, W. K.; Kwong, T. N.; Lo, N. W.; Ip, M.; Wong, S. H.; Sung, J. J. Y.; Chiu, P. W. Y.; Zhang, L. Real-Time Tracking of Fluorescent Magnetic Spore−Based Microrobots for Remote Detection of *C. Diff*. *Toxins. Sci. Adv.* **2019**, *5*, No. eaau9650.
(134) Kim, S.; Qiu, F.; Kim, S.; Ghanbari, A.; Moon, C.; Zhang, L.; Nelson, B. J.; Choi, H. Fabrication and Characterization of Magnetic Microrobots for Three-Dimensional Cell Culture and Targeted Transportation. *Adv. Mater.* **2013**, *25*, 5863−5868.
(135) Li, J.; Li, X.; Luo, T.; Wang, R.; Liu, C.; Chen, S.; Li, D.; Yue, J.; Cheng, S.-h.; Sun, D. Development of a Magnetic Microrobot for Carrying and Delivering Targeted Cells. *Sci. Rob.* **2018**, *3*, No. eaat8829.
(136) Jeon, S.; Kim, S.; Ha, S.; Lee, S.; Kim, E.; Kim, S. Y.; Park, S. H.; Jeon, J. H.; Kim, S. W.; Moon, C.; Nelson, B. J.; Kim, J.-Y.; Yu, S.-W.; Choi, H. Magnetically Actuated Microrobots as a Platform for Stem Cell Transplantation. *Sci. Rob.* **2019**, *4*, No. eaav4317.
(137) Go, G.; Jeong, S.-G.; Yoo, A.; Han, J.; Kang, B.; Kim, S.; Nguyen, K. T.; Jin, Z.; Kim, C.-S.; Seo, Y. R.; Kang, J. Y.; Na, J. Y.; Song, E. K.; Jeong, Y.; Seon, K. K.; Park, J.-O.; Choi, E. Human Adipose−Derived Mesenchymal Stem Cell-Based Medical Micro-

robot System for Knee Cartilage Regeneration *In Vivo*. *Sci. Rob.* **2020**, *5*, eaay6626.
(138) Park, J.; Jin, C.; Lee, S.; Kim, J.-Y.; Choi, H. Magnetically Actuated Degradable Microrobots for Actively Controlled Drug Release and Hyperthermia Therapy. *Adv. Healthcare Mater.* **2019**, *8*, 1900213.
(139) Ceylan, H.; Yasa, I. C.; Yasa, O.; Tabak, A. F.; Giltinan, J.; Sitti, M. 3D-Printed Biodegradable Microswimmer for Theranostic Cargo Delivery and Release. *ACS Nano* **2019**, *13*, 3353−3362.
(140) Van de Walle, A.; Sangnier, A. P.; Abou-Hassan, A.; Curcio, A.; Hemadi, M.; Menguy, N.; Lalatonne, Y.; Luciani, N.; Wilhelm, C. Biosynthesis of Magnetic Nanoparticles from Nano-Degradation Products Revealed in Human Stem Cells. *Proc. Natl. Acad. Sci. U. S. A.* **2019**, *116*, 4044−4053.
(141) Mazuel, F.; Espinosa, A.; Luciani, N.; Reffay, M.; Le Borgne, R.; Motte, L.; Desboeufs, K.; Michel, A.; Pellegrino, T.; Lalatonne, Y.; Wilhelm, C. Massive Intracellular Biodegradation of IRON Oxide Nanoparticles Evidenced Magnetically at Single-Endosome and Tissue Levels. *ACS Nano* **2016**, *10*, 7627−7638.
(142) Foroozandeh, P.; Aziz, A. A. Insight into Cellular Uptake and Intracellular Trafficking of Nanoparticles. *Nanoscale Res. Lett.* **2018**, *13*, 339.
(143) Sangnier, A. P.; Van de Walle, A. B.; Curcio, A.; Le Borgne, R.; Motte, L.; Lalatonne, Y.; Wilhelm, C. Impact of Magnetic Nanoparticle Surface Coating on Their Long-Term Intracellular Biodegradation in Stem Cells. *Nanoscale* **2019**, *11*, 16488−16498.
(144) Laskar, A.; Ghosh, M.; Khattak, S. I.; Li, W.; Yuan, X.-M. Degradation of Superparamagnetic IRON Oxide Nanoparticle-Induced Ferritin by Lysosomal Cathepsins and Related Immune Response. *Nanomedicine* **2012**, *7*, 705−717.
(145) Curcio, A.; Van de Walle, A.; Serrano, A.; Preveral, S.; Péchoux, C.; Pignol, D.; Menguy, N.; Lefèvre, C. T.; Espinosa, A.; Wilhelm, C. Transformation Cycle of Magnetosomes in Human Stem Cells: From Degradation to Biosynthesis of Magnetic Nanoparticles Anew. *ACS Nano* **2020**, *14*, 1406.
(146) Pernal, S.; Wu, V. M.; Uskoković, V. Hydroxyapatite as a Vehicle for the Selective Effect of Superparamagnetic IRON Oxide Nanoparticles against Human Glioblastoma Cells. *ACS Appl. Mater. Interfaces* **2017**, *9*, 39283−39302.
(147) Mazuel, F.; Espinosa, A.; Radtke, G.; Bugnet, M.; Neveu, S.; Lalatonne, Y.; Botton, G. A.; Abou-Hassan, A.; Wilhelm, C. Magneto-Thermal Metrics Can Mirror the Long-Term Intracellular Fate of Magneto-Plasmonic Nanohybrids and Reveal the Remarkable Shielding Effect of Gold. *Adv. Funct. Mater.* **2017**, *27*, 1605997.
(148) Esteban-Fernández de Ávila, B.; Angsantikul, P.; Li, J.; Gao, W.; Zhang, L.; Wang, J. Micromotors Go *In Vivo*: From Test Tubes to Live Animals. *Adv. Funct. Mater.* **2018**, *28*, 1705640.
(149) Srivastava, S. K.; Medina-Sánchez, M.; Koch, B.; Schmidt, O. G. Medibots: Dual-Action Biogenic Microdaggers for Single-Cell Surgery and Drug Release. *Adv. Mater.* **2016**, *28*, 832−837.
(150) Wu, Z.; Troll, J.; Jeong, H.-H.; Wei, Q.; Stang, M.; Ziemssen, F.; Wang, Z.; Dong, M.; Schnichels, S.; Qiu, T.; Fischer, P. A Swarm of Slippery Micropropellers Penetrates the Vitreous Body of the Eye. *Sci. Adv.* **2018**, *4*, No. eaat4388.
(151) Hadjikhani, A.; Rodzinski, A.; Wang, P.; Nagesetti, A.; Guduru, R.; Liang, P.; Runowicz, C.; Shahbazmohamadi, S.; Khizroev, S. Biodistribution and Clearance of Magnetoelectric Nanoparticles for Nanomedical Applications Using Energy Dispersive Spectroscopy. *Nanomedicine* **2017**, *12*, 1801−1822.
(152) Pané, S.; Puigmartí-Luis, J.; Bergeles, C.; Chen, X.-Z.; Pellicer, E.; Sort, J.; Počepcová, V.; Ferreira, A.; Nelson, B. J. Imaging Technologies for Biomedical Micro- and Nanoswimmers. *Adv. Mater. Technol.* **2019**, *4*, 1800575.
(153) Medina-Sánchez, M.; Schmidt, O. G. Medical Microbots Need Better Imaging and Control. *Nature* **2017**, *545*, 406.
(154) Aziz, A.; Medina-Sánchez, M.; Claussen, J.; Schmidt, O. G. Real-Time Optoacoustic Tracking of Single Moving Micro-Objects in Deep Phantom and *Ex Vivo* Tissues. *Nano Lett.* **2019**, *19*, 6612−6620.
(155) Aziz, A.; Medina-Sánchez, M.; Koukourakis, N.; Wang, J.; Kuschmierz, R.; Radner, H.; Czarske, J. W.; Schmidt, O. G. Real-Time IR Tracking of Single Reflective Micromotors Through Scattering Tissues. *Adv. Funct. Mater.* **2019**, *29*, 1905272.
(156) Hu, S.; Eberhard, L.; Chen, J.; Love, J. C.; Butler, J. P.; Fredberg, J. J.; Whitesides, G. M.; Wang, N. Mechanical Anisotropy of Adherent Cells Probed by a Three-Dimensional Magnetic Twisting Device. *Am. J. Physiol. Cell Physiol.* **2004**, *287*, C1184−C1191.
(157) Roca-Cusachs, P.; Del Rio, A.; Puklin-Faucher, E.; Gauthier, N. C.; Biais, N.; Sheetz, M. P. Integrin-Dependent Force Transmission to the Extracellular Matrix by α-Actinin Triggers Adhesion Maturation. *Proc. Natl. Acad. Sci. U. S. A.* **2013**, *110*, E1361−E1370.
(158) Lee, J.-H.; Kim, J.-w.; Levy, M.; Kao, A.; Noh, S.-h.; Bozovic, D.; Cheon, J. Magnetic Nanoparticles for Ultrafast Mechanical Control of Inner Ear Hair Cells. *ACS Nano* **2014**, *8*, 6590−6598.
(159) Zablotskii, V.; Lunov, O.; Dejneka, A.; Jastrabik, L.; Polyakova, T.; Syrovets, T.; Simmet, T. Nanomechanics of Magnetically Driven Cellular Endocytosis. *Appl. Phys. Lett.* **2011**, *99*, 183701.
(160) Kunze, A.; Murray, C. T.; Godzich, C.; Lin, J.; Owsley, K.; Tay, A.; Di Carlo, D. Modulating Motility of Intracellular Vesicles in Cortical Neurons with Nanomagnetic Forces On-Chip. *Lab Chip* **2017**, *17*, 842−854.
(161) Tseng, P.; Judy, J. W.; Di Carlo, D. Magnetic Nanoparticle−Mediated Massively Parallel Mechanical Modulation of Single-Cell Behavior. *Nat. Methods* **2012**, *9*, 1113.

https://dx.doi.org/10.1021/acsnano.0c00959
ACS Nano 2020, 14, 3805−3821